

# **HEIMDALL**

## The God of Surveillance



**Department of Aerospace Engineering  
Indian Institute of Technology Kanpur  
Kanpur India 208016  
June 1, 2017**

# INDIAN INSTITUTE OF TECHNOLOGY KANPUR



Department of Aerospace Engineering  
Indian Institute of Technology Kanpur  
Kanpur, India 208016



## HEIMDALL The God of Surveillance

In Response to 34<sup>th</sup> Annual American Helicopter Society  
International Student Design Competition - Undergraduate Student Category  
Team Nimbus - June 1, 2017

---

Sourav Kumar Sinha - Team Leader,  
Undergraduate Student,  
[srvsinha@iitk.ac.in](mailto:srvsinha@iitk.ac.in)  
Contact no: +91-9005358851

Mendu Rama Krishna, UG Student

---

Pokar Monil, UG Student

---

Animesh Kumar Shastry, UG Student

Dr. Abhishek - Faculty Advisor

All students received academic credit for AE 660 "Preliminary Design of Helicopter" through submission of this design proposal.



**INDIAN INSTITUTE OF TECHNOLOGY KANPUR**  
**DEPARTMENT OF AEROSPACE ENGINEERING**

Indian Institute of Technology Kanpur,  
Kanpur, India 208016

In Response to 2017 American Helicopter Society  
Student Design Competition - Undergraduate Category

Pursued as a course project for credited course  
AE 660A: Preliminary Design of Helicopter

January 30, 2017  
Team: **Nimbus**

*Sourav-Sinha*

Sourav Kumar Sinha - **Team Leader**,  
Undergraduate Student,  
srvsinha@iitk.ac.in  
Contact no: +91-9005358851

*M.Ramabirshna*

Mendu Rama Krishna,  
Undergraduate Student,  
rkrishna@iitk.ac.in

*Animesh*

Animesh Kumar Shastry,  
Undergraduate Student,  
animeshs@iitk.ac.in

*Monil*

Pokar Monil,  
Undergraduate Student,  
monilp@iitk.ac.in

*Abhishek*

Dr. Abhishek - **Faculty Advisor**,  
abhish@iitk.ac.in

## Acknowledgements

Team Nimbus would like express it's sincere thanks of gratitude to **Prof. C. Venkatesan**, Professor, Department of Aerospace Engineering, Indian Institute of Technology Kanpur for his inputs and feedback during the entire design process and for teaching the Helicopter Theory (AE 686) course which helped us learn about the basics of helicopter aerodynamics.

We are highly indebted to **Ms. Kirti Bhatnagar**, Project Associate, for her continuous guidance and help in CAD drawing work. We would also like to thank the graduate students, of Micro Air Vehicle Lab IIT Kanpur, **Mr. Rahul R.**, **Mr. Ramdas Gadekar**, **Mr. Karthik S.** and **Mr. Naba Kishore Routray** for numerous discussion which helped us during the design exercise.

# Contents

<b>1</b>	<b>Introduction</b>	<b>1</b>
<b>2</b>	<b>Configuration Selection</b>	<b>1</b>
2.1	Mission Profile . . . . .	1
2.2	Evaluation Method . . . . .	1
2.3	Design Drivers . . . . .	1
2.4	Candidate Configurations . . . . .	3
2.5	Configuration Rating . . . . .	5
2.6	Final Configuration Selection . . . . .	6
<b>3</b>	<b>Preliminary Sizing</b>	<b>8</b>
3.1	Design Requirements . . . . .	8
3.2	Description of Algorithm . . . . .	8
3.3	Trade Studies . . . . .	9
3.3.1	Blade Loading Coefficient . . . . .	10
3.3.2	Rotor Solidity . . . . .	11
3.3.3	Tip Speed . . . . .	13
3.4	Refined Weight Analysis . . . . .	13
3.5	Engine Selection . . . . .	14
3.5.1	Choice of Type of Engine . . . . .	15
3.5.2	Final Selection . . . . .	15
3.6	Preliminary Sizing Results . . . . .	16
<b>4</b>	<b>Energy Harvesting System</b>	<b>19</b>
<b>5</b>	<b>Rotor System Design</b>	<b>21</b>
5.1	Hinge Offset . . . . .	21
5.2	Blade Root Cutout . . . . .	21
5.3	Inter-rotor Spacing . . . . .	22
5.4	Airfoil Selection . . . . .	22
5.5	Blade Twist . . . . .	23
5.5.1	Upper Rotor Blade Twist . . . . .	24
5.5.2	Lower Rotor Blade Twist . . . . .	24
5.6	Blade Taper . . . . .	25
5.7	Blade Tip Geometry . . . . .	25
5.8	Dissimilar Radius . . . . .	25
5.9	Optimized Results for Heimdall . . . . .	27
5.10	Rotor Blade Structural Design . . . . .	29
5.10.1	Material Selection . . . . .	29
5.10.2	D-Spar . . . . .	30
5.10.3	Blade construction . . . . .	30
5.11	Hub Design . . . . .	30
<b>6</b>	<b>Drive Train</b>	<b>31</b>
6.1	Transmission system configuration . . . . .	31

<b>7 Airframe Design</b>	<b>33</b>
7.1 Structural Details . . . . .	33
7.1.1 Transmission and Powerplant Deck . . . . .	34
7.1.2 Fuel Tank . . . . .	34
7.2 Crashworthiness . . . . .	34
7.3 Material selection . . . . .	34
7.4 V-Nz plot . . . . .	35
<b>8 Landing Gear Design</b>	<b>35</b>
8.1 Landing Gear Classification . . . . .	36
8.1.1 Skid vs Wheel Type Landing Gear . . . . .	36
8.2 Landing Gear Selection . . . . .	36
8.2.1 Retractable vs Non-retractable Landing Gear . . . . .	36
8.3 Static Stability Angle Analysis . . . . .	36
8.4 Structure Analysis . . . . .	38
<b>9 Drag Estimation</b>	<b>38</b>
9.1 Parasitic Drag . . . . .	38
9.2 Vertical Drag . . . . .	38
<b>10 Forward Flight</b>	<b>39</b>
10.1 Performance Analysis . . . . .	39
<b>11 Stability Analysis</b>	<b>42</b>
11.1 Lateral and Longitudinal Modes . . . . .	42
11.2 Tail Sizing . . . . .	43
<b>12 Avionics</b>	<b>43</b>
12.1 Autonomous Flight Navigating System . . . . .	43
12.1.1 Motion Planning System . . . . .	43
12.1.2 Flight Control System . . . . .	44
12.1.2.1 Control Law . . . . .	44
12.2 Health and Usage Monitoring System (HUMS) . . . . .	46
<b>13 Weight Analysis</b>	<b>46</b>
13.1 Weight Estimation . . . . .	46
<b>14 Cost Analysis</b>	<b>49</b>
14.1 Acquisition Cost . . . . .	49
14.2 Reasons for low cost . . . . .	49
<b>15 Conclusion</b>	<b>50</b>

## List of Figures

1	Mission Profile	2
2	Singlecopter	5
3	Validation of BEMT model for conventional configuration	7
4	Validation of BEMT model for coaxial configuration	7
5	Power vs. thrust comparison between conventional and coaxial rotors with identical blade properties	8
6	Flow chart for preliminary sizing	10
7	Variation of gross take-off weight with blade loading coefficient ( $C_T/\sigma$ )	11
8	variation of blade loading with rotor blade collective pitch	11
9	Variation of rotor diameter with number of blades	12
10	Variation of fuel weight with number of blades	12
11	Variation of GTOW with number of blades and AR	12
12	Variation of fuel weight with aspect ratio	12
13	Variation of empty weight, fuel weight and GTOW with hover tip speed	13
14	Variation of rotor diameter with hover tip speed	14
15	Variation of power with hovering flight time with the baseline engine	14
16	Zoche-02A Engine	16
17	Variation of blade loading coefficient with chord for determining chord length	17
18	Variation of thrust coefficient with hovering time for the final design	17
19	Variation of Blade Loading with hovering time for the final design	17
20	Variation of Power required with hovering time for the final design	18
21	Variation of Weight with hovering time for the final design	18
22	Angle of attack variation over the blade operating at a blade loading of 0.115	18
23	Angle of attack variation over the blade operating at a blade loading of 0.06	18
24	Rotor blade sectional properties	22
25	Pitching moment coefficient distribution for SC 1095 and SC 1095 R8	23
26	Lift/Drag distribution for SC 1095 and SC 1095 R8	23
27	Variation of $C_T$ vs. $C_P$ as a function of blade twist rate on upper rotor	24
28	AOA distribution over upper blade during take-off for different blade twist	24
29	AOA distribution over lower blade during take-off for different blade twist	25
30	Variation of $C_T$ vs. $C_P$ as a function of blade twist rate on lower rotor	25
31	Variation of $C_T$ vs. $C_P$ for different values of dissimilar radius factor	26
32	AOA distribution over lower blade during take-off for dissimilar radius optimization	26
33	AOA distribution over upper blade during take-off for dissimilar radius optimization	27
34	Blade loading versus chord distribution for the optimized design	27
35	Variation of Weight with hovering time for the optimized design	28
36	Variation of required power with hovering time for the optimized design	28
37	Variation of figure of merit with the blade loading	29
38	V-Nz plot for Heimdall	35
39	Stress Plot on the landing gear	38
40	Trim algorithm for forward flight performance prediction	40
41	Control Angles at different forward speeds	40
42	Power required at different forward speeds	40
43	Attitude at different forward speeds	41

44	Endurance at different forward speeds . . . . .	41
45	Range at different forward speeds . . . . .	41
46	Rate of Climb at different forward speeds . . . . .	41
47	Eigen value plot for Longitudinal Hover Stability . . . . .	42
48	Eigen value plot for Lateral Hover Stability . . . . .	42
49	Autonomous Flight Navigation System Architecture . . . . .	45
50	Control Architecture Block Diagram . . . . .	46

## List of Tables

1	<i>Preference scale for Analytic Hierarchy Process</i>	3
2	<i>Relative ranking of design drivers and finalized weightage obtained using AHP</i>	4
3	<i>Configuration selection matrix obtained using AHP</i>	6
4	<i>Summary of rotors with identical blade properties</i>	7
5	<i>Heimdall design alternatives for candidate engine choices</i>	16
6	<i>Output of the preliminary sizing for Heimdall</i>	17
7	<i>Power generation using different energy harvesting methods</i>	21
8	<i>Rotor preliminary design parameters</i>	21
9	<i>Relative hub clearances of Kamov helicopters [11]</i>	22
10	<i>Rotor optimized design parameters</i>	28
11	<i>Properties of materials used in the blade manufacturing</i>	30
12	<i>Transmission gear specifications</i>	33
13	<i>Component drag breakdown</i>	39
14	<i>Eigenvalues for Coupled Hover Stability</i>	42
15	<i>Weight of individual subsystems of Heimdall</i>	47
16	<i>Cost of individual subsystems of Heimdall</i>	50

## List of Symbols

- A: Rotor Disc Area
- AR: Aspect Ratio
- c: Chord
- $V_{tip}$ : Tip Speed
- $C_T/\sigma$ : Blade Loading
- $\sigma$ : Solidity
- L/D: Lift to Drag Ratio
- $\Omega$ : Rotor Speed
- $\alpha$ : Angle of Attack
- $C_l$ : Airfoil Lift Coefficient
- $C_d$ : Airfoil Drag Coefficient
- a: Lift Curve Slope
- $C_{d_o}$ : Airfoil Profile Drag Coefficient
- $N_b$ : Number of Blades
- R: Blade Radius
- $C_T$ : Thrust Coefficient
- $C_P$ : Power Coefficient
- h: Rotor Spacing
- M: Mach Number
- $\theta_{o1}$ : Upper Rotor Blade Collective Angle
- $\theta_{o2}$ : Lower Rotor Blade Collective Angle
- $\theta_s$ : Longitudinal Cyclic Pitch
- $\theta_c$ : Lateral Cyclic Pitch
- p: Roll Rate
- q: Pitch Rate
- r: Yaw Rate

- l: Rolling Moment
- m: Pitching Moment
- n: Yawing Moment
- $\beta$ : Sideslip Angle

## List of Abbreviations

- **AFCS** : Automatic Flight Control System
- **AHP** : Analytical Hierarchy Process
- **AHS** : American Helicopter Society
- **AOA** : Angle of Attack
- **APU** : Auxiliary Power Unit
- **BEMT** : Blade Element Momentum Theory
- **BET** : Blade Element Theory
- **BL** : Blade Loading
- **CCW** : Counter Clockwise
- **CG** : Center of Gravity
- **CPU** : Central Processing Unit
- **CW** : Clockwise
- **DL** : Disc Loading
- **FADEC** : Full Authority Diesel Engine Control
- **GPS** : Global Positioning System
- **GW** : Gross Weight
- **GTOW** : Gross Take-off Weight
- **HERS** : Home Energy Rating System
- **IC** : Internal Combustion
- **MEMS** : Micro Electro Mechanical System
- **MSL** : Mean Sea Level
- **OGE** : Out-of-Ground Effect
- **OPOC** : Opposed Piston Opposed Cylinder
- **RFP** : Request For Proposal
- **RPM** : Revolution Per Minute
- **SC** : Sikorsky

- **SFC** : Specific Fuel Consumption
- **SLAM** : Simultaneous Localization and Mapping
- **UAV** : Unmanned Aerial Vehicle
- **VHF** : Very High Frequency

# 1 Introduction

This design document describes the conceptual design of the Heimdall, a coaxial rotor design with high hover efficiency designed specifically for high endurance missions. The design was developed in response to the Request for Proposals (RFP) for the American Helicopter Society (AHS) Student Design Competition sponsored by Sikorsky Aircraft Corporation. The RFP identified the need for a helicopter with the ability to hover for 24 hours while still demonstrating other typical helicopter attributes. It also has to carry 176.4 lbs (80 kg) of payload during the entire duration of flight. A helicopter with 24 hour hover endurance does not exist. Therefore, the design requirements pose serious challenge towards designing a hovering vehicle that can sustain such long duration flight while being safe and reliable at the same time. This report presents a cost effective design that meets and even exceeds all the RFP requirements, while incorporating mature, feasible technology to ensure great chance of mission success.

## 2 Configuration Selection

This section discusses the tradeoff study involved in the final aircraft configuration selection. The evaluation methods employed to arrive at the selection are discussed systematically.

### 2.1 Mission Profile

The RFP demands the aircraft to hover for a cumulative duration of 24 hours inside three separate hover stations following takeoff without landing. Therefore the main design driver is high hovering efficiency. During hover the aircraft must be supported exclusively by aerodynamic forces, and must have near zero relative velocity with respect to a ground observer station, both longitudinally and laterally with no change in altitude. It is also required that during hover, the aircraft must fly out-of-ground-effect at an altitude of at least twice the largest vehicle dimension and also the wind speed must be under 9.71 kt (5m/s). The hover station volume has been specified as that of sphere of 20 m radius. The three hover stations are at least 0.54 nm (1 km) apart, as measured from their respective centroids. The complete mission profile is summarized in Fig. 1.

### 2.2 Evaluation Method

Analytical Hierarchy Process (AHP), a tool commonly used for multi-criteria decision making, is used to develop the selection matrix. The AHP method is based on three principles: first, prioritization of the parameters; second, comparative judgment of the alternatives for all the parameters individually; third, synthesis of the priorities for the alternatives. For determining priority, often AHP uses standard preference table like the one given in Table 1. These standards have been determined on considerable basis in comparing two or more alternatives.

### 2.3 Design Drivers

In this section a fundamental set of critical design drivers are established from a combination of design philosophy and the design requirements expressed in the RFP. The design drivers would later be



Figure 1: Mission Profile

prioritized using Analytical Hierarchy Process (AHP), developed by Saaty [1]. The design drivers identified are listed below along with a brief description.

- **Hovering Efficiency:** Hovering efficiency represented in the form of power loading (thrust/power) is probably the most critical design parameter towards efficient design of rotor for 24 hours hovering requirement laid by the RFP. Higher the hovering efficiency, higher would be the endurance of the aircraft for a given weight and fuel volume.
- **Empty Weight Fraction:** Given the weight of payload by the RFP, lower empty fraction would imply less power consumption for a given all up weight allowing for increased fuel capacity which eventually results in improved endurance.
- **Power Loss Due to Anti-Torque (AT) System:** The anti-torque system consumes a significant amount of the available power (10 to 20% for conventional single main rotor design). Therefore, the anti-torque generation mechanism with least power loss would be the most desirable.
- **Compactness:** The aircraft performing the mission is required to fit in the given hover station volume. Overall, the compactness of the design would allow for use of larger rotors which would decrease the disc loading and enhance hover efficiency. However, the hover volume specified by the RFP is a sphere of 20 meter radius, which is probably large enough to accommodate several large helicopters.
- **Low Speed Manoeuvrability:** Since the hover is the dominant portion of the mission profile and the total distance covered in forward flight is merely 3 km which would be possible covered

Level of importance	Definition
1	Equally important
3	Moderately more important
5	Strongly more important
7	Very strongly more important
9	Extremely more important
2,4,6,8	Intermediate more important
Inverse	If x has one value when compared with y, then y has the inverse (reciprocal) value of it when compared to x

Table 1: *Preference scale for Analytic Hierarchy Process*

at slow speeds to prevent overshooting the hover stations, good low speed manoeuvrability is a desired feature. This would also ensure that the helicopter can maintain its position within the hover station with accuracy.

- **Technical Maturity:** Use of unproven technology in the design decreases the reliability. Technical Maturity however restricts the innovation in the design. RFP requires the proposed design solution to be ready in 3-4 years for production, therefore maturity of the configuration is also considered.
- **Cruise Efficiency:** Cruise at higher L/D ratio will lead to higher endurance. It is desirable feature for every flight vehicle. However, for the current design it is given significantly low priority as the forward flight duration is insignificant in comparison to hovering flight.

These design drivers are ranked after doing the pairwise comparison using AHP method keeping in mind the requirements for 24 hour endurance. The finalized weightage of each design driver is presented in Table 2, which would be used for comparing different potential configurations. Certain other parameters like **operational safety**, **downwash** and **autorotation capability** were also considered, but were not of significance for the mission profile specified. The helicopter is required to hover at a height equal to twice of the largest dimension of the vehicle, which may put the condition in the Dead Man's Curve area, where the height available may not be enough to enter autorotation.

## 2.4 Candidate Configurations

The design drivers considered to meet the requirements of the RFP can be achievable with only a limited number of configurations. First, all the well known vehicle configurations which are traditionally known to have good hovering characteristics were considered as a candidate. In addition, some innovative new concepts were also proposed for comparative study. After this, thorough analysis was carried out before the candidates were ranked. The following candidate configuration were listed for detailed analysis and comparison.

- **Coaxial Contra-rotating:** A co-axial helicopter consists of two main rotor systems mounted co-axially on a single axis. This type of configuration does not require a separate anti-torque device and offers maximum compactness. For a coaxial rotor, yawing moment equilibrium is

<b>Design Drivers</b>	Hovering Efficiency	Empty Weight Fraction	Power Loss to AT System	Compactness	Low Speed Maneuverability	Technical Maturity	Cruise Efficiency	<b>Weightage</b>
Hovering Efficiency	1.00	2.00	4.00	7.00	6.00	5.00	7.00	37.5 %
Empty Weight Fraction	0.50	1.00	3.00	6.00	5.00	4.00	6.00	26.5 %
Power Loss to AT System	0.25	0.33	1.00	4.00	3.00	2.00	4.00	13.5%
Compactness	0.14	0.17	0.25	1.00	0.50	0.33	1.00	3.8 %
Low Speed Maneuverability	0.17	0.20	0.33	2.00	1.00	0.50	2.00	5.9 %
Technical Maturity	0.20	0.25	0.50	3.00	2.00	1.00	3.00	9.1%
Cruise Efficiency	0.14	0.17	0.25	1.00	0.50	0.33	1.00	3.8 %

Table 2: *Relative ranking of design drivers and finalized weightage obtained using AHP*

achieved by matching the torque of the upper and lower rotors via differential collective pitch input so that the net torque about the rotor axis is zero. The inherent compactness of the configuration (lack of tail rotor) can allow for larger individual rotors with low disc loadings and high hover efficiency which can possibly overcome the losses due to the aerodynamic interference between the two rotors.

- **Conventional:** The conventional helicopter consists of a single main rotor with an anti-torque device such as conventional tail-rotor, fenestron or NOTAR system. Tail rotor power loss can be 10–15% of the total power and it doesn't contribute in rotor thrust.
- **Singlecopter:** It consists of a single main rotor and vanes below it as shown in the Fig. 2. In this configuration vanes are used as an anti-torque device, the torque required to compensate the rotor reaction is generated by deflecting the vanes in the rotor downwash. The loss in power for this case is due to the drag (profile and pressure) generated by the vanes. This also results in increased thrust requirement from main rotor.
- **Tandem:** The tandem helicopter consists of two main rotor systems situated at the front and rear end of the fuselage. This configuration doesn't need an anti-torque system. However, it has two separate rotor hubs and the rotors may or may not have region of interference. It would typically have higher empty weight due to requirement for powering two equal rotors. It sacrifices compactness and therefore, to meet the dimensional constraints, it would result in smaller rotors with higher disc loading and therefore, lower hover efficiency. It should be noted that side-by-side helicopter configuration is not considered separately as the tandem and side-by-side configurations are identical for hovering flight.
- **Synchropter:** The synchropter helicopter uses the intermeshing rotor concept. The two main rotor shafts are positioned at some angle to provide sufficient clearance. The rotor blades are phased by some angle through the transmission system to prevent the blades from striking each

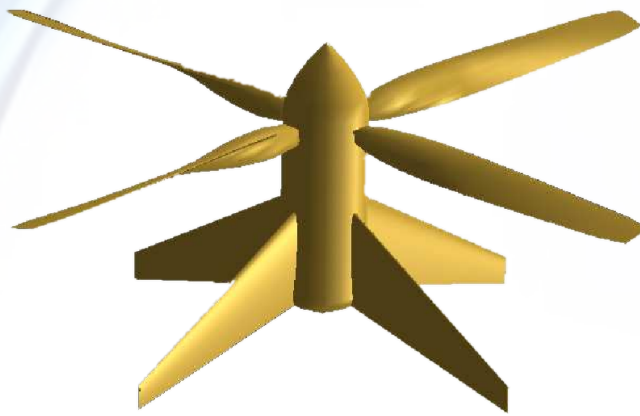


Figure 2: Singlecopter

other. This configuration doesn't require an anti-torque device but has two separate hubs, and part of the rotor wake interferes with other rotor.

- **Ducted Multirotor:** The ducted multirotor (four to six rotors) consists of multiple rotors which are mounted along different axes. Use of multiple rotors divides the thrust requirement making them small and rigid, therefore ducts can be put around them to increase their efficiency. There is no need of anti-torque device for this configuration. The moment due the individual rotors will nullify among themselves by having different directions of rotation of the rotors.
- **Ducted Coaxial:** It is same as the co-axial configuration, but will consist of a duct around the rotors. This addition of ducts around the rotors have both advantages and disadvantages. Use of ducts would rule out the use of swashplate based control and would require use of vanes or other devices for primary control.

## 2.5 Configuration Rating

Based on the RFP requirements and the typical characteristics of the individual configurations listed above, a pairwise comparison is made and the candidate configurations are ranked using AHP. The weightage of design drivers listed in Table 2 are used for arriving at the final score of the candidate configurations, which is shown in Table 3. The AHP based ranking rejected ducted multirotor and tandem (also side-by-side) configurations as the most unsuited configurations for this mission. This was expected because these configurations lack in high hover efficiency and low empty weight requirements which are the most critical drivers for the mission.

The top three configurations identified are conventional, coaxial and singlecopter configurations. The yaw control of the singlecopter design would require large vanes which would need to be supported with structure that would penalize the design by creating very high parasite drag in cruise flight. With the wake of the rotor getting blown downstream in forward flight, the achievement of anti-torque during forward motion would be very challenging, the design also eliminates possibility of horizontal and vertical stabilizers which would further complicate the stability of the vehicle in forward flight. Due to these challenges and relative immaturity of the singlecopter concept, it is not considered for further analysis. The conventional and coaxial designs have very close score and hence are studied closely to finalize the candidate configuration.

Candidate Configurations	Hovering Efficiency	Empty Weight Fraction	Power Loss to AT System	Compactness	Low Speed Manoeuvrability	Technical Maturity	Cruise Efficiency	Total Score
<i>Weightage</i>	0.375	0.265	0.135	0.038	0.059	0.091	0.038	
Conventional	0.25	0.18	0.10	0.06	0.24	0.22	0.27	0.20
Coaxial Contra-rotating	0.14	0.30	0.17	0.25	0.24	0.22	0.26	0.21
Synchropter	0.14	0.18	0.17	0.17	0.24	0.22	0.17	0.17
Tandem	0.05	0.04	0.06	0.04	0.06	0.22	0.10	0.07
Ducted Multirotor	0.08	0.02	0.04	0.03	0.04	0.05	0.04	0.053
Ducted Coaxial	0.11	0.08	0.17	0.36	0.04	0.03	0.05	0.11
Singlecopter	0.22	0.18	0.29	0.09	0.14	0.03	0.10	0.19

Table 3: Configuration selection matrix obtained using AHP

## 2.6 Final Configuration Selection

The coaxial design has the advantages of low empty weight and compactness over the conventional helicopter. The conventional configuration is superior from a hover efficiency point of view, however the tail rotor consumes additional 10 % - 15 % of the main rotor power to maintain yaw moment equilibrium. Both these designs appear to have comparable hover efficiency and empty weight and hence can only be separated based on quantitative comparison.

To get a clearer picture of the better choice for the RFP, a quantitative hover performance comparison is carried out using a Blade Element Momentum Theory (BEMT) model developed for this purpose. The BEMT analysis is used to model the coaxial and conventional helicopter configuration to estimate the total power requirement for each of the competing configurations. To check the numerical accuracy of the simulation, the model was first validated using the single and coaxial rotor data for Harrington's Rotor 2 [3]. The validation of predicted results using the BEMT for conventional configuration is shown in Fig. 3 and for coaxial rotor is shown in Fig. 4. The predictions show excellent correlation with experimental results for Harrington's Rotor 2 with 25 ft (7.62 m) diameter and untwisted blades. The rotor, having a tip speed of 392 ft/s, had two blades that were tapered only in thickness-to-chord ratio with a solidity of 0.076 for single rotor (i.e.,  $2\sigma = 0.152$  as a coaxial) and had a inter-rotor spacing of 0.16 R. For the validation, the sectional blade aerodynamic characteristics were taken as a function of sectional angle of attack i.e., by using

$$C_d = C_{d_o} + d_1\alpha + d_2\alpha^2$$

$$C_l = a\alpha$$

where  $d_1 = 0.021$ ,  $d_2 = 0.65$ ,  $C_{d_o} = 0.011$  and  $a = 5.73$  are based on NACA0012 airfoil section measurements [4].

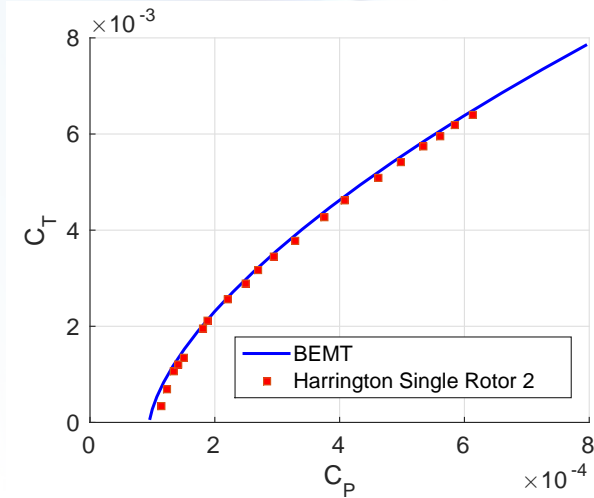


Figure 3: Validation of BEMT model for conventional configuration

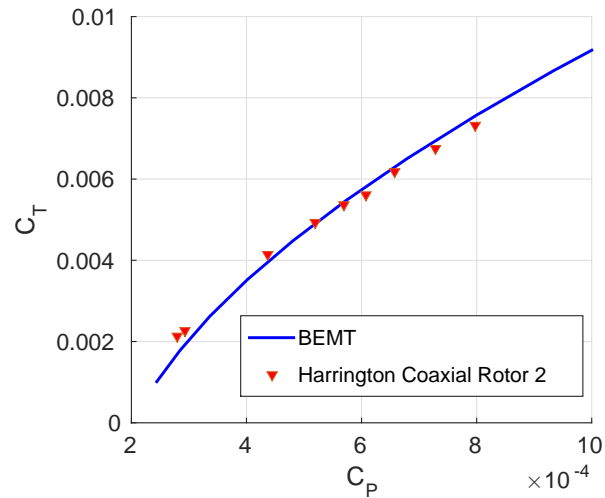


Figure 4: Validation of BEMT model for coaxial configuration

A fair comparison between a coaxial and conventional helicopter can be made only when the difference lies only in parameters which distinguish both the configurations, namely the distance between the rotors and sense of rotation of the blades. Any difference should arise only because of the differences of the blade aerodynamic interactions for coaxial rotor, the rotor-vane interaction for single copter and the power required by tail rotor for conventional configuration. To make consistent comparison between conventional and coaxial rotors, the approach suggested by Brown et al. [5] is used. Therefore, the Harrington Rotor 2 (coaxial) is compared to an equivalent conventional rotor having same number of total blades (i.e. four) and same blade geometry (see Table 4 for details of rotor configurations). For simplification, the tail rotor power consumption for the conventional configuration is directly taken as 10% of the main rotor power for the conventional helicopter case as suggested by [5].

	Harrington Rotor 2 (coaxial)	Equivalent Conventional
Radius	3.81m	3.81m
Number of Rotors	2	1
Blades per Rotor	2	4
Root Chord	0.4572m	0.4572m
Tip Speed	119.48 m/s	119.48 m/s
Airfoil section	NACA 0012	NACA 0012

Table 4: Summary of rotors with identical blade properties

From Fig. 5, it is concluded that the total power required to hover for the conventional helicopter configuration is always higher than that of an equivalent coaxial helicopter. Therefore, the coaxial configuration is identified to be the best possible solution for designing a helicopter with 24 hour hover endurance.

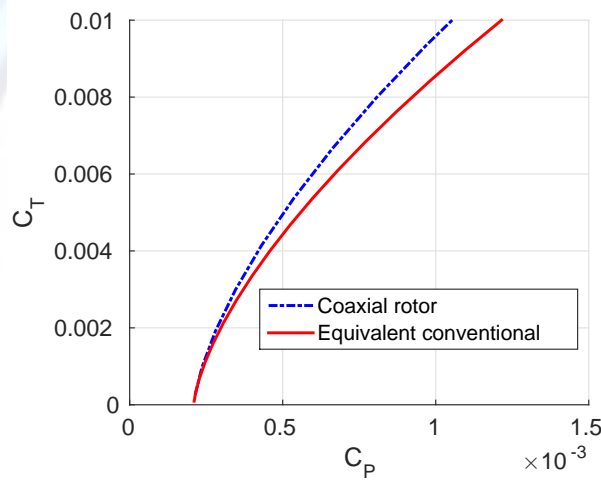


Figure 5: Power vs. thrust comparison between conventional and coaxial rotors with identical blade properties

### 3 Preliminary Sizing

The aim of the preliminary sizing is to obtain the design parameters that meet the requirements specified by the RFP. Heimdall is designed to be a light weight, low disk loading, extremely efficient hovering vehicle. The overall size of the design is determined in terms of Gross weight (GW), number of blades, rotor solidity, tip speed and power requirements. In addition, the component weights are estimated using a methodology developed by Prouty [6]. Trade studies are performed to select the optimum values of all the design parameters.

#### 3.1 Design Requirements

Reiterating the mission requirements, the proposed vehicle should have a capability of hovering for 24 hrs under out-of-ground effect (OGE) carrying a non-productive payload of 80 kg the entire time. OGE is defined as an altitude at least twice the largest vehicle dimension (i.e. approximately 50 - 100 m above ground). As permitted by the RFP, the design calculations are performed based on the rotor and engine performance at mean sea level (MSL) conditions.

#### 3.2 Description of Algorithm

The design analysis uses an iterative process, starting with the specification of mission requirements laid by the RFP, such as the required hover time, forward flight capability and payload. In the next step, a number of parameters that are not given explicitly in the mission requirements, such as the propulsive system, transmission efficiency, rotor blade sectional characteristic, etc are initialized. The propulsion system of weight 300 kg and a conservative engine SFC of  $0.38 \frac{\text{lbs}}{\text{hphr}}$  is assumed, based on the preliminary information given in the RFP. A conservative transmission efficiency of 90% is considered. NACA 0012 airfoil is taken as the blade airfoil for calculations done at this stage. These initial parameters would be updated subsequently to arrive at the final design. The flow of the design methodology is depicted in the Fig. 6. The design variables that are considered for the sizing include

blade loading coefficient, number of blades, aspect ratio and tip speed. The entire process of sizing estimation was run for various combinations of these design variables doing a trade study to select the best (lightest, most efficient) design.

For these design variables, a reasonable estimate of fuel weight is assumed as an initial guess, following which the empty weight is calculated, resulting in an estimate of gross take-off weight. The critical part of initial sizing step involves careful accounting for the effect of change in the weight of the vehicle with time, due to the weight of fuel consumed during 24 hrs flight. Neglecting the effect of weight change due to consumption of fuel results in gross overestimate of fuel required, which results in higher empty weight which in turn increases power required and then fuel weight required in an iterative manner, resulting in failure of the design process. Therefore, after estimating the gross take-off weight, the calculation of power required and fuel consumed is done in a continuous loop with weight of fuel remaining updated for every minute of flight time, allowing for the reduction in gross weight and the power required with each step of the loop accounting for the fuel getting consumed. After 24 hours of flight time, the leftover fuel is subtracted from the initial fuel weight estimate and the whole step following the fuel weight estimation is repeated until remaining fuel weight of 5-10 lbs (extra fuel) is achieved. This allowed for accurate estimation of amount of fuel required and also resulted in realistic estimate of power required. The power required for initial sizing for coaxial rotor configuration is estimated using momentum theory formula for coaxial rotor available in [7].

### 3.3 Trade Studies

To achieve the most efficient design solution for the helicopter, the critical parameters that affect the hovering performance and weight of the helicopter are varied to arrive at the lightest and most efficient helicopter. The said parameters are disc loading ( $\frac{T}{A}$ ), rotor solidity ( $\sigma$ ) and blade loading coefficient ( $\frac{C_T}{\sigma}$ ). In the trade studies, the variation in rotor solidity, disc loading, blade loading coefficient is obtained by changing the aspect ratio ( $\frac{R}{c}$ ), number of blades ( $N_b$ ) and hover tip speed ( $V_{tip}$ ). For designing a hover efficient helicopter, we needed to minimize the disk loading which is achieved by maximizing the aspect ratio. However, increasing the aspect ratio increases the rotor size, empty weight and also the profile power. Tip speed needs to be reduced to control the increase in profile power. Finally, an optimal compromise has to be established.

Another important parameter for the current design is the choice of the engine. State-of-the-art turbine and piston engines, as well as some emerging engine concepts were considered for selection of an engine with the lowest possible specific fuel consumption, which directly governs the all up weight of the vehicle. This study is conducted in two parts. The preliminary analysis is performed to obtain design predictions using engine data based on average power-to-weight ratio and specific fuel consumption (SFC) for generic engines. This part of the analysis is useful in examining the effect of changing various design parameters and selecting the best configuration in terms of number of blades and rotor solidity for different engine cases. The estimated power requirements are then used to aid in the selection of actual off-the-shelf engine. Then, a final analysis is performed using the actual data for the selected engine to size each configuration for systematic comparison.

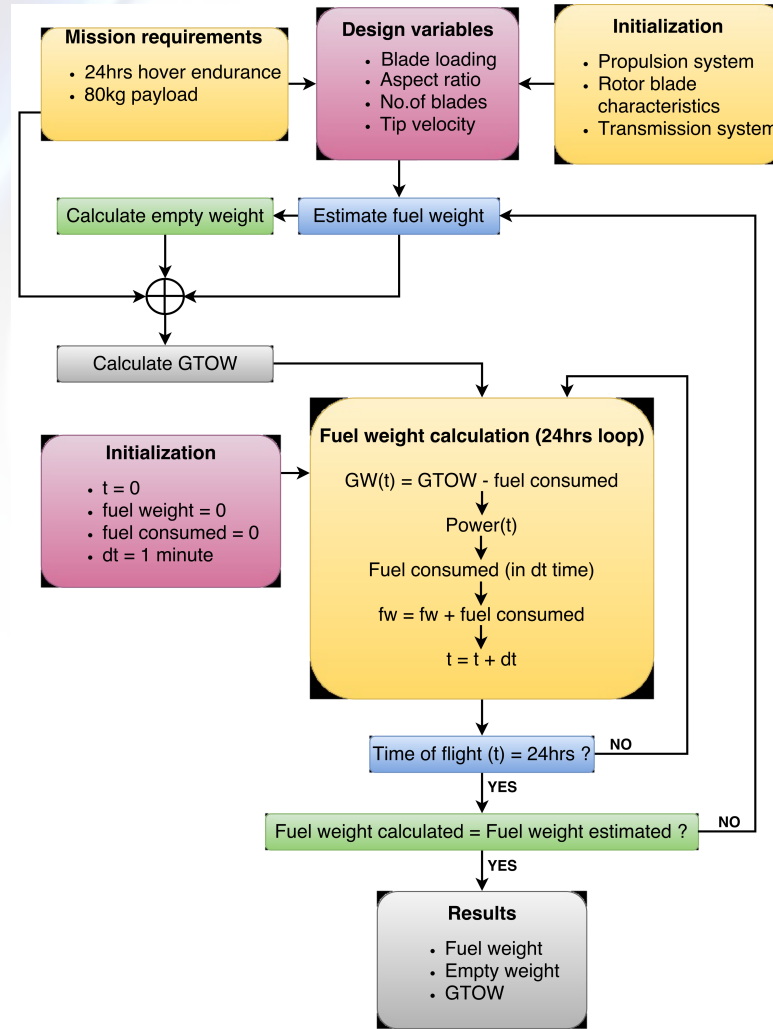


Figure 6: Flow chart for preliminary sizing

### 3.3.1 Blade Loading Coefficient

The most important factor that influences the choice of blade loading coefficient is the blade stall margin during hover. Increasing blade loading causes a reduction in the overall weight up to a minimum, after which it starts to increase again as shown in Fig. 7. Increase in blade loading also increases the blade collective pitch required for flight. Different design alternatives are generated with same number of blades (2 blades per rotor), aspect ratio (23) and tip speed (450 ft/sec). Since there are no requirements for specific high maneuverability and rate of climb during the initial phase of the mission, the maximum blade loading coefficient is fixed to a value that results in the collective pitch of lower blade to be around  $12^\circ$ . This implies that the operating angle of attack for both top and bottom rotor is significantly less than  $12^\circ$  inboards which is reasonably low than the stall limit. Thereby, the design offers adequate stall margin for the initial stage of the mission. With passage of time, the weight of the helicopter decreases which brings down the requirement for collective even further. Hence, a blade loading coefficient ( $C_T/\sigma$ ) of 0.115 is chosen Fig. 8 for Heimdall keeping the required lower rotor collective pitch at take-off equal to  $12^\circ$ . The collective requirement decreases with forward flight, therefore, possibility of onset of stall may not occur. To further avoid blade stall during forward

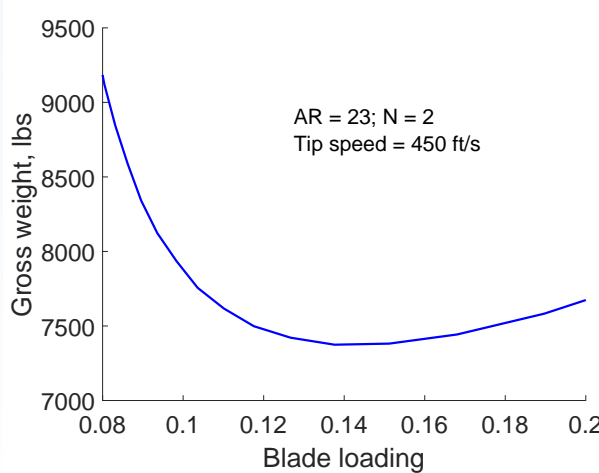


Figure 7: Variation of gross take-off weight with blade loading coefficient ( $C_T/\sigma$ )

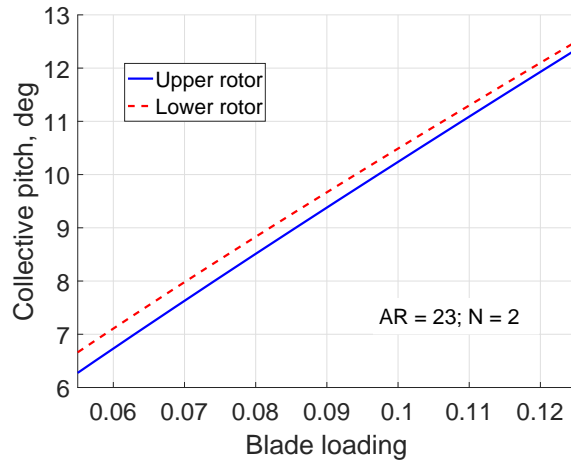


Figure 8: variation of blade loading with rotor blade collective pitch

flight, the movement from the first station to the second hover station may be done after several hours, so that the weight and hence the blade collective requirement has reduced to a smaller value by that time.

### 3.3.2 Rotor Solidity

The variation in rotor solidity is achieved by changing the number of blades and the aspect ratio.

$$\sigma = \frac{N_b}{\pi AR}$$

where  $\sigma$  denotes solidity per rotor ( $\sigma_{tot} = 2\sigma$ ),  $N_b$  denotes the number of blades per rotor and AR denotes the aspect ratio.

- **Number of Blades:**

After fixing the value of blade loading, trade studies are done to obtain the number of blades per rotor. During this study, the aspect ratio (23), blade loading coefficient (0.115) and hover tip speed (450 ft/s) are kept constant. With the above parameters held constant, an increase in number of blades

1. increases the rotor solidity, which in turn increases the disk loading which can be seen from the function,  $DL = \sigma BL \rho V_{Tip}^2$
2. reduces the rotor diameter Fig. 9, which reduces the empty weight and hence the total weight

The increase in disc loading in turn increases the induced power, which increases the fuel weight Fig. 10 and hence total weight.

Hence, the total weight is a balance between these two contradicting factors. From Fig. 11 we can see that for a given AR, tip speed and blade loading the gross take-off weight is minimum for 2-bladed rotor. Hence, the number of blades for Heimdall rotors are fixed at two.

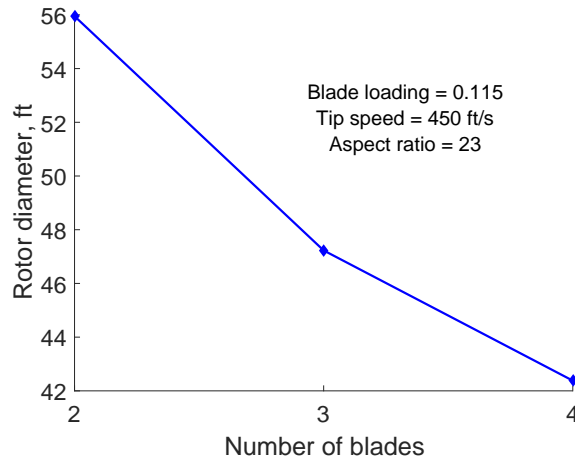


Figure 9: Variation of rotor diameter with number of blades

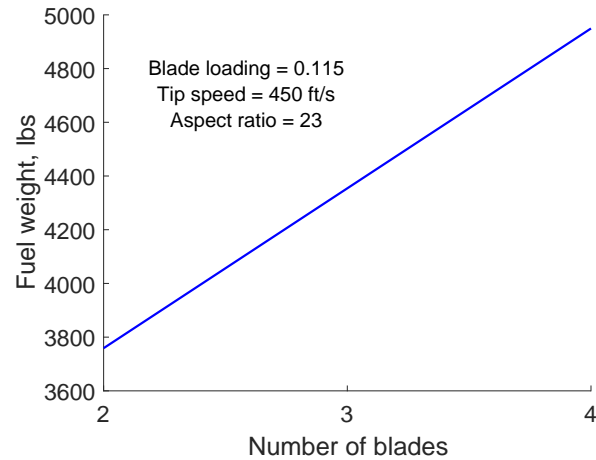


Figure 10: Variation of fuel weight with number of blades

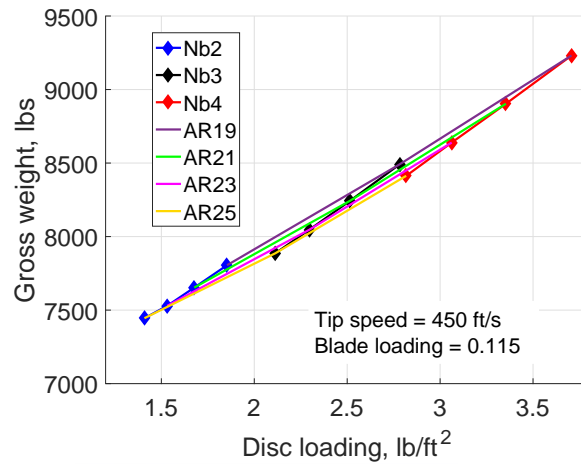


Figure 11: Variation of GTOW with number of blades and AR

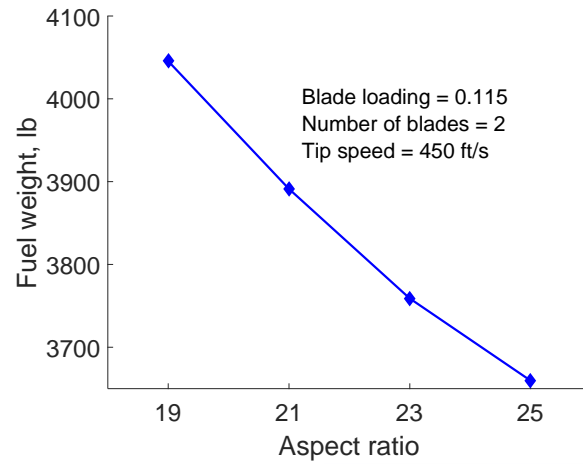


Figure 12: Variation of fuel weight with aspect ratio

- Aspect Ratio:**

After finalizing the number of blades and blade loading, design alternatives are generated to select the aspect ratio. In this study, AR was varied from 19 to 25, keeping  $N_b$ , blade loading and tip speed constant. Increasing aspect ratio, decreases the disk loading, which results in reduction of induced power, which in turn reduces the GTOW weight Fig. 11 due to reduction of fuel weight Fig. 12. However, high aspect ratio also results in very large diameter with smaller chord. Therefore, considering the structural and aerodynamic limitations of high aspect ratio, aspect ratio of 23 was chosen for the design. This is somewhat higher than typical for helicopters, but seems to reduce the design weight significantly.

### 3.3.3 Tip Speed

In this trade study, the tip speed of the rotor is varied from 300 ft/s to 700 ft/s for fixed  $N_b$  (2), aspect ratio (23) and blade loading (0.115). The variation in empty weight, fuel weight, and GTOW with tip speed with above parameters kept constant is shown in Fig. 13. The variation in rotor diameter with tip speed is also shown in Fig. 14. The reduction in tip speed leads to an increase in the rotor diameter to keep the blade loading constant, which causes an increase in the empty weight of the helicopter Fig. 13. But at the same time it also decreases the disc loading, which deceases the power required, leading to the reduction of fuel weight. Hence, gross take-off weight achieved is a balance of these two factors. Although tip speed of 350 ft/s corresponds to the lowest GTOW, tip speed of 450 ft/s was chosen for Heimdall to maintain minimum level of autorotative performance by maintaining the stored kinetic energy of the rotor to a reasonable limit.

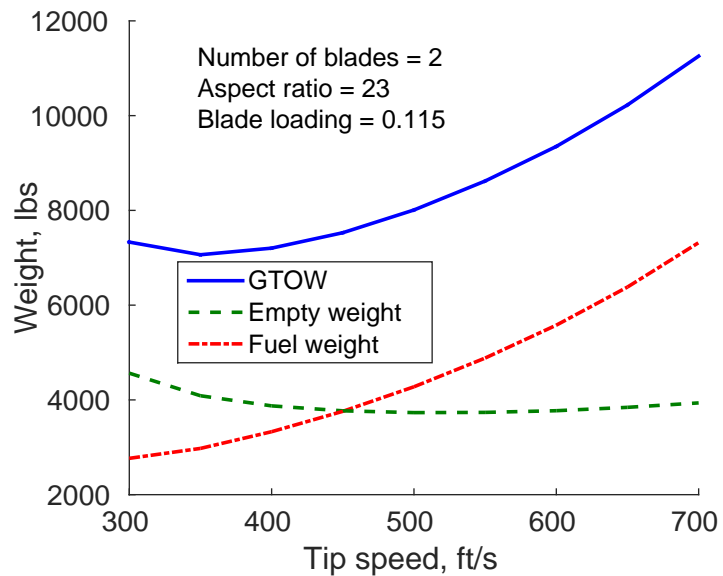


Figure 13: Variation of empty weight, fuel weight and GTOW with hover tip speed

The major issue with decreasing hover tip speed is the retreating blade stall during forward flight, and autorotative capability. But then again, autorotation is not critical for the mission and Heimdall is not required to fly at higher speeds for the current mission hence retreating blade stall is not a major concern.

### 3.4 Refined Weight Analysis

After the design variables were fixed, some refinements in the traditional weight analysis is done to adapt it for the modern UAV design. The modifications include:

1. 100 lbs of weight is added in empty weight calculation to account for the auxiliary power unit (APU).
2. 20 hp power is included for running the APU.
3. Weight of drive system is updated to 200 kg based on detailed analysis.

4. Weight contribution of hydraulics and cockpit controls are discarded from the empty weight calculation as they are not required for the design. A telemetry system is to be used for display of flight parameters on the ground station instead of cockpit controls.
5. 10 minutes of extra flight time is taken into account for estimation of reserve fuel for weight calculation.
6. 10 % transmission loss is considered for rotor power calculation.

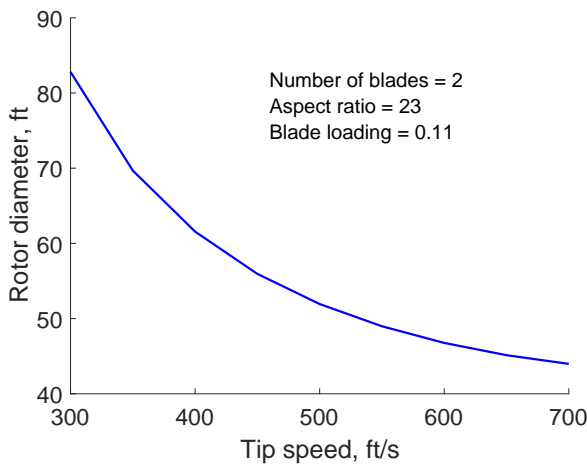


Figure 14: Variation of rotor diameter with hover tip speed

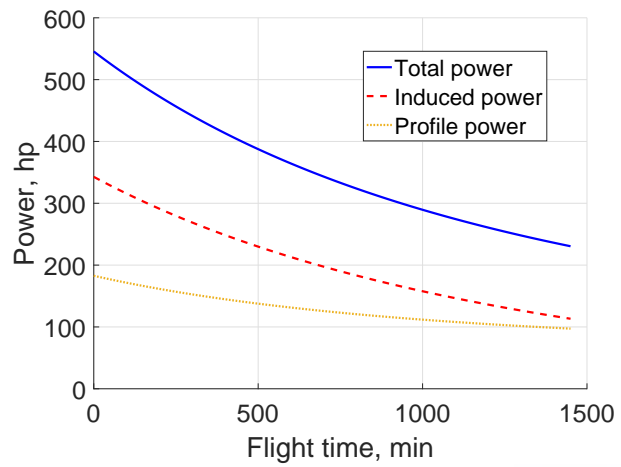


Figure 15: Variation of power with hovering flight time with the baseline engine

**Use of Composite Materials** The design formulas given by Prouty are based upon helicopters with metallic structures. Some modifications have been incorporated in these formulas for calculating the weight of components made of advance materials like composites, etc. Use of composite materials gives lower weight as compared to the weight calculated using Prouty's formula. The weight of rotor blades, hub, and electrical system are reduced by 6%, 30% and 15% respectively as per recommendations from [8]. The weight of the airframe is reduced by almost 25% [9]. With this updated weight analysis, the power required during the hovering flight time Fig. 15 for the selected configuration ( $N_b = 2$ ,  $AR = 23$ ,  $BL = 0.115$  and  $V_{tip} = 450\text{ft/s}$ ) is then calculated which is used in the next section for the selection of engine for Heimdall . More of these updating in weight and power optimization is explored in the upcoming sections to optimize the vehicle weight even further.

### 3.5 Engine Selection

The choice of engine is a very important design variable for the current mission. The requirement for hovering for 24 hours rules most electric propulsion concepts out. The electric propulsion systems powered by batteries would not loose weight with passage of time as no mass can be ejected from the system at anytime during the 24 hour flight. With the current state of energy density for batteries, the weight of the batteries is going to be significantly high compared to a fossil fuel based powerplant. This has been confirmed in a recent study from NASA [10],which concluded that for a pure helicopter type vehicle, the possibility of having improved performance using electric or hybrid concepts is not

possible, even with 20-30 years advanced electrical technology. The endurance, range and loiter duration all reduces with use of electrical or hybrid concepts.

Therefore, the default choice for Heimdall is a fuel engine. The choice of light weight engine with low specific fuel consumption that can generate the power required for Heimdall and can help reduce the weight of the fuel and thereby, the final GTOW significantly. From the preliminary analysis, the power required with the baseline configuration was estimated to be 550 hp approximately, as shown in Fig. 15. The power required decreases further if we a lighter engine with lower SFC is used. Hence, different off-the-shelf light engines which offer minimum SFC with max power output in the range of 400-650 hp were explored. The search resulted various modern diesel engines as prime candidates for powering Heimdall , as they offered lowest SFC ranging from 0.33-0.40 lb/hp-hr in their weight class. Also, modern diesel engines are environment friendly, reliable, robust with relatively high power densities. The BSFCs of the diesel engines is of the order of 0.33-0.40 lb/hp-hr, which is superior to the best average of 0.45-0.50 lb/hp-hr for gasoline aero-engines. Some advanced helicopter turboshaft engines (e.g., GEs CT7-8) may reach at an optimum operational set-point equivalent BSFC of 0.451 lb/hp-hr at maximum continuous power of 2155 hp with dry weight of 543 kg. Existing enabling technologies when employed would make aero-diesel superior to even gasoline engine and a tough competitor to light-to-medium turboshafts and turboprop engines.

### 3.5.1 Choice of Type of Engine

Modern helicopter gasoline reciprocating engines (e.g., Lycoming engines for Robinson, Enstrom and Sikorsky/Schweizer light helicopters) normally have power by weight ratio of about 0.6 hp/lb with SFC of the order of 0.5 lb/hp-hr. Diesel-aero engines achieve 10-20% better power by weight ratio with half of the SFC. The power by weight ratio of modern helicopter turboshafts is about quadruple, while the SFC is on the same order of the gasoline engines. Accordingly, for higher horsepower applications ( $\geq$  400 hp), turboshafts are clearly technically superior to gasoline engines. However, the total purchasing, operational, maintenance costs and more complex turbine operations need to be considered as well. On the other hand, aero-diesels have low purchase and maintenance cost (same as gasoline or lower) while delivering superior BSFC compared to turboshafts. While the gasoline engines can only use Aviation gasoline and turboshaft mostly only JP fuels, aero-diesels can use cheaper diesel as well as widely available jet fuels (JP-4, JP-5). A turboshaft engine is essentially normally-aspirated engine losing power with altitude. For example, at 10,000 feet pressure altitude a Rolls Royce turboshaft would deliver only about 74% of its rated power, while turbocharged IC diesel engines would still deliver 100% of its rated power, being well below its critical altitudes.

### 3.5.2 Final Selection

Aero-diesels are the new kid on the block in the world of aviation propulsion and have, in our opinion, bright future. Diesels deliver highest efficiency of all existing practical heat-conversion engines. They are reliable, robust, and safe and have some clear advantages over gasoline engines in terms of higher efficiencies, higher performance figures, flight safety, and fire safety due to combustion of heavier low-flammability fuels. The use of environmentally friendlier bio-diesels and cheaper jet fuels is easily accommodated. Combined with the custom-designed FADECs, single-unit aero-diesels can be produced today in the range of 50 to 2,000 hp to cover the operating range of light-to-medium airplanes and helicopters. Aero-diesels are also becoming engines of choice for UAVs. Particularly, a combination of aero-diesel with the HERS power-assist system could offer attractive advantages to

helicopters all but eliminating no-mans land in Height-Velocity (H/V) curve and increasing service altitudes. It is not difficult to imagine that within the next 30 years half of the IC reciprocating aero-engines worldwide will be diesel.

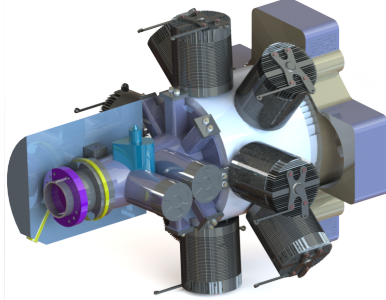


Figure 16: Zoche-02A Engine

Following this study, it is decided to go on with diesel engine. The two models Zoche 02A and EM100 (OPOC) are the best candidates having minimum weight and lower SFC. However, two units of Zoche engines are required as it delivers maximum power of 300 hp per unit. From the final comparison, shown in Table 5, it is observed that Zoche gives better design with lesser gross weight. Hence, Zoche O2A is selected as the engine for Heimdall . Use of two engine design also improves safety of the design, as even with one engine failure, the helicopter may be able to perform controlled landing under certain conditions. This is also aids the current design, for which the autorotational capability has been sacrificed for the desire of more efficient hovering rotor.

	<b>EM100 (OPOC)</b>	<b>Zoche 02A (radial engine)</b>
SFC (lb/hp/hr)	0.34	0.346
Power Rating (hp)	650	300
Installed Weight (lb)	700	335
Units Required	1	2
GTOW (lb)	6014	5778
Empty Weight (lb)	2917	2835
Fuel Weight (lb)	2921.3	2767
Max Power (hp)	526	508

Table 5: *Heimdall design alternatives for candidate engine choices*

### 3.6 Preliminary Sizing Results

Based on the justified trade studies done in the previous sections, the complete weight analysis is done for the selected configuration ( $N_b = 2$ ,  $AR = 23$ ,  $BL = 0.115$  and  $V_{tip} = 450\text{ft/s}$ ) with Zoche O2A radial engine using BEMT analysis (validated earlier) developed for the design. For the above choice of parameters, the chord length of 1.05 ft is found suitable for maintaining blade loading coefficient of 0.115 during take-off as shown in Fig. 17. This corresponds to a moderate hover  $C_T$  of 0.0064 at the beginning of the mission which nearly halves to  $C_T$  of 0.0033 at the end of 24 hours as shown in Fig. 18. Corresponding variation in  $C_T/\sigma$  is shown in Fig. 19. The variation of power and weight with hovering time are shown in Figs. 20 and 21 respectively.

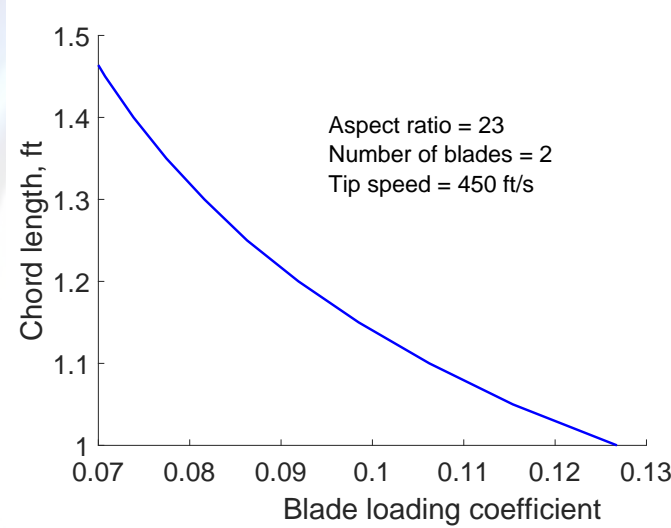


Figure 17: Variation of blade loading coefficient with chord for determining chord length

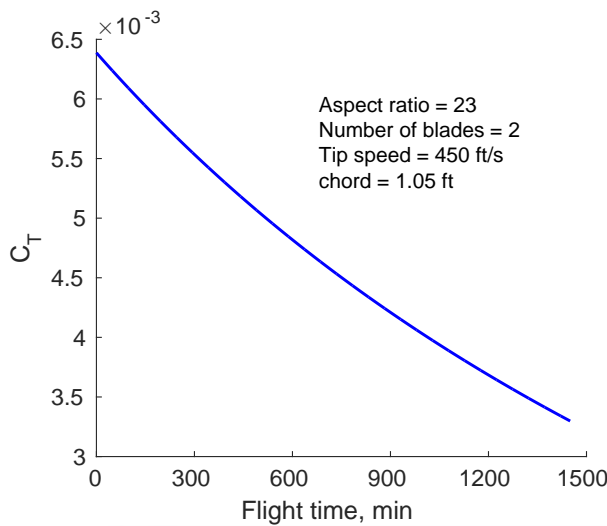


Figure 18: Variation of thrust coefficient with hovering time for the final design

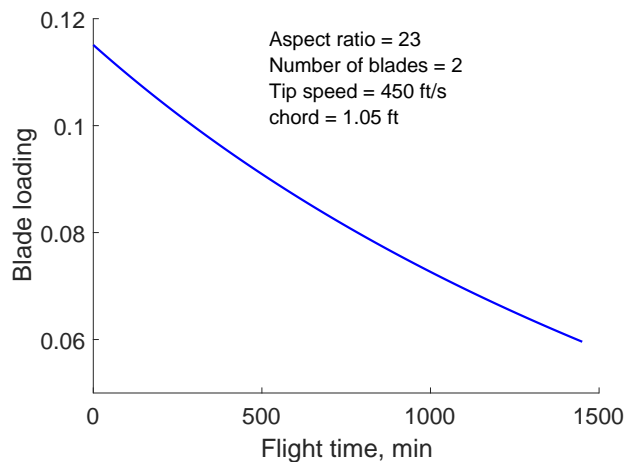


Figure 19: Variation of Blade Loading with hovering time for the final design

The summary of the parameters identified from preliminary sizing carried out for Heimdall is shown in Table 6.

N <sub>b</sub>	AR	Tip Speed	$\sigma_{tot}$	Radius	Chord	GTOW	Powerplant	Max Power
2	23	450 ft/s	0.0554	24.15 ft	1.05 ft	5617 lbs	2*Zoche O2A	474 hp

Table 6: Output of the preliminary sizing for Heimdall

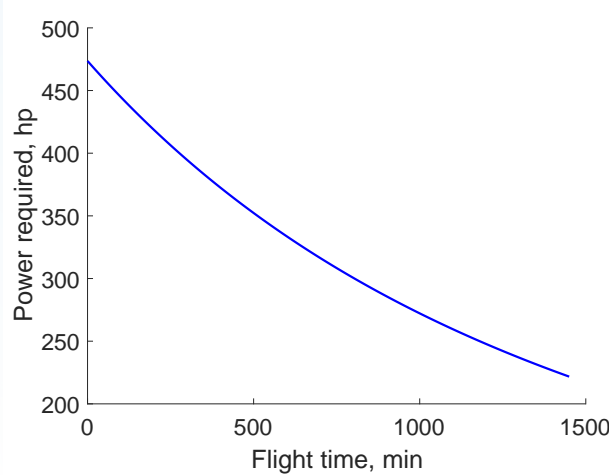


Figure 20: Variation of Power required with hovering time for the final design

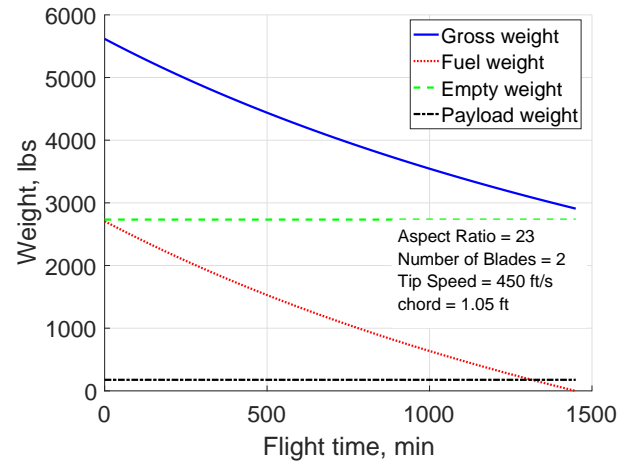


Figure 21: Variation of Weight with hovering time for the final design

From Fig. 19 it is observed that blade loading of the helicopter varies from 0.115 to approximately 0.06 during the 24 hour flight duration. The blade collective requirement decreases with time from  $12^\circ$  to around  $7.5^\circ$  as shown in Fig. 8. The other major concern is that no part of the rotor blade should produce negative lift (negative angle of attack) during the entire period of 24 hours.

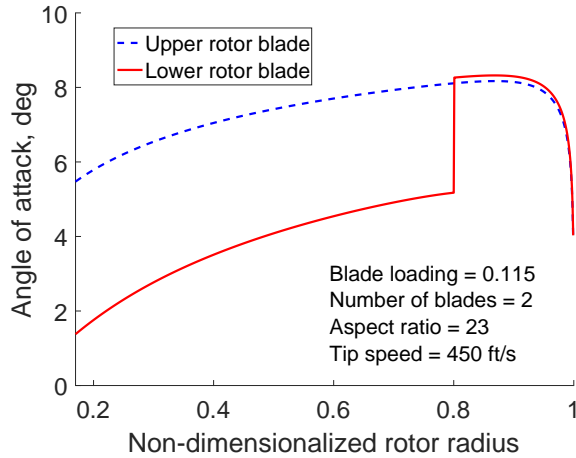


Figure 22: Angle of attack variation over the blade operating at a blade loading of 0.115

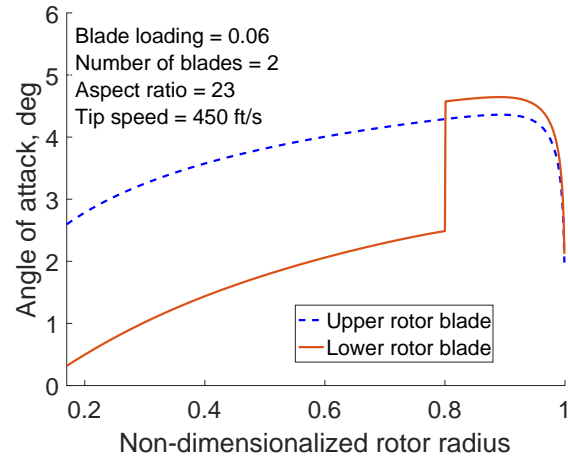


Figure 23: Angle of attack variation over the blade operating at a blade loading of 0.06

To ensure this, the predicted angle of attack distribution is plotted using the BEMT analysis for two different blade loading cases corresponding to just after take-off ( $BL = 0.115$ ) and just before landing ( $BL = 0.06$ ). From Figs. 22 and 23 it is concluded that no part of the blade operates under negative angle of attack and the blade angle of attack is less than  $8^\circ$  which is below stall limit for typical rotorcraft airfoils.

## 4 Energy Harvesting System

This section explores the different methods of energy harvesting. Energy harvesting would be instrumental in missions which requires endurance since power supply through different sources may reduce the required fuel weight of the Heimdall thus increasing the empty weight fraction. Harvesting mechanical energy is an important route in obtaining cost-effective, clean and sustainable electric energy. We may tap energy from following energy harvesting sources:

- Inductive energy harvesting form variable frequency
- Downwash loss
- Heat generated in the gearbox
- Solar energy

Following are the conditions, we have considered in evaluating various energy harvesting technology applicability in our design:

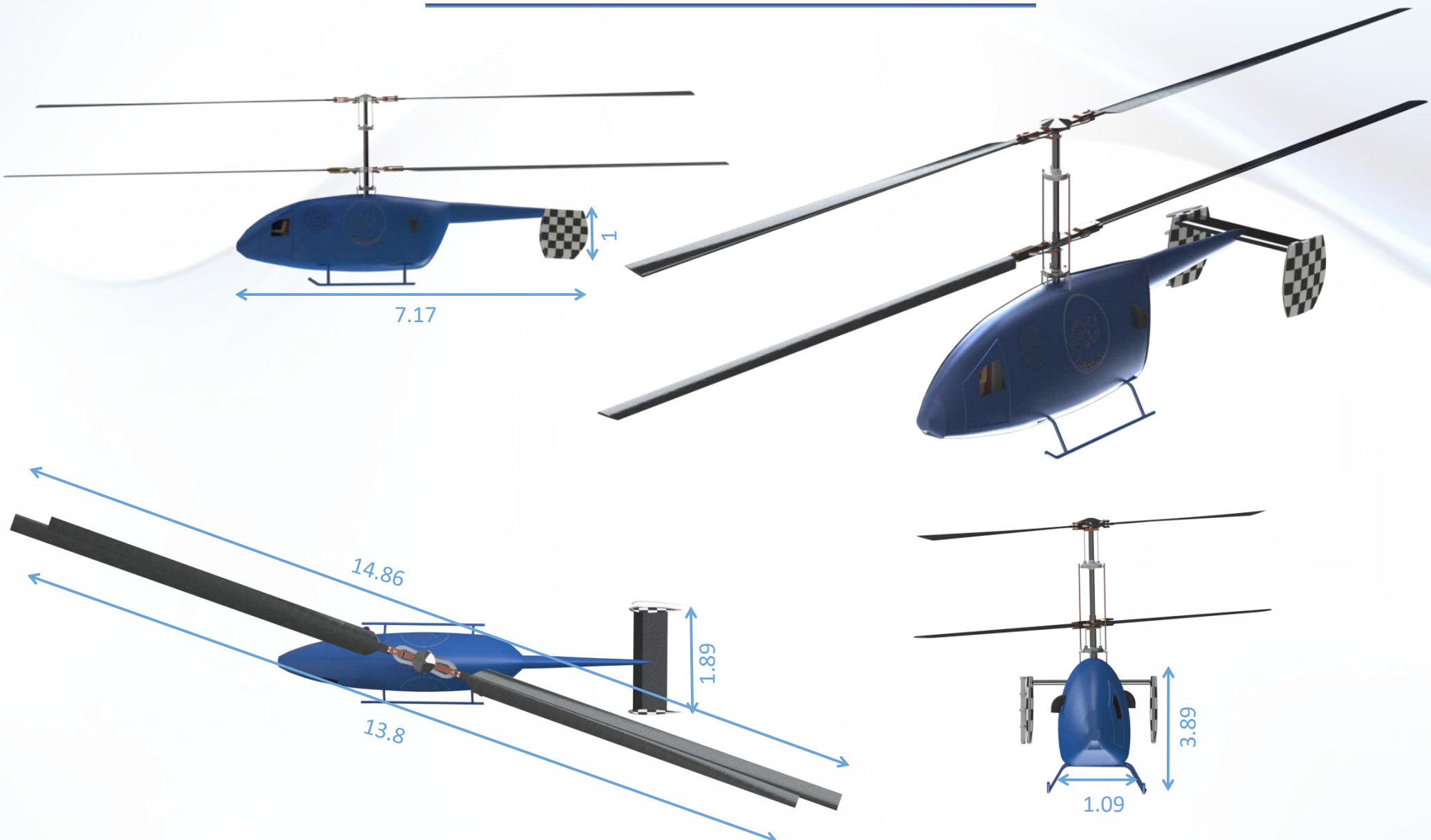
- **Complexity :** It includes system cost, challenges in installations, number of complimentary components, weight of the system
- **Robustness :** Capability to withstand extreme on-board conditions like vibrations, high temperatures, wind dust
- **Power Output :** To be able to generate power that can suffice our requirements.

Energy harvesters convert non-electrical energy to electricity. We have investigated following technologies that will act as a generator harvesting kinetic energy using electromagnetic induction, piezoelectricity, Triboelectrification that convert friction to electricity.

1. **Piezoelectric generators :** Piezoelectric materials are commonly used to generate electricity from vibrations due to the simple conversion from mechanical to electrical domain. Piezoelectric harvesters mainly rely on resonance at a specific frequency. This limits the applicability of the harvester, also the power output would be lower than 1mW.
2. **Electromagnetic generators:** Electromagnetic induction harvesters are composed of a magnetic source and coil that are in relative motion to each other. Electromagnetic generators are a mature technology as most of the electrical energy in the power grids is generated using this technology.
3. **Triboelectric generators:** If the stationary and rotating system are in close proximity to each other, a triboelectric harvester could be used. Triboelectric harvesters convert friction between objects into electrical charges. Triboelectric generator can effectively harness various ambient motions, including light wind, tap water flow and normal body movement.

Such technologies can be used to power on board wireless sensors in rotating environment but installing such devices, lets say Triboelectric generators, would also increase weight of the helicopter, so additional power must be needed to lift that weight, thus amount of energy generated from harvesters is getting consumed due to increased requirement for lift. Therefore, these technologies do not meet the requirements of current mission, as they did not produce enough power with our defined conditions.

# Heimdall Airframe 4-view



All dimensions in metres

**Foldout 1**

Type of Technology	Power Generated (mW)
Piezoelectric	0.18
Electromagnetic	5.6
Triboelectric	300

Table 7: Power generation using different energy harvesting methods

## 5 Rotor System Design

The rotors of the Heimdall are designed for efficient hover performance at sea level conditions. The rotor diameter, number of blades, chord length, aspect ratio, tip speed and required thrust coefficient were previously selected / estimated in the preliminary sizing study (see section 3.6). Both the rotor are contra-rotating, rotating at same angular velocity with upper rotor rotating in counter clockwise (CCW) direction and lower rotor in clockwise (CW) direction

	Upper Rotor	Lower rotor
Aspect Ratio	23	23
No. of Blades	2	2
Blade Chord	0.32 m (1.05 ft)	0.32 m (1.05 ft)
Tip Speed	137.16 m/s (450 ft/s)	137.16 m/s (450 ft/s)

Table 8: Rotor preliminary design parameters

### 5.1 Hinge Offset

Higher hinge offset increases the control moment of the helicopter. However, the manoeuvrability requirements from the current design are not very critical. Hence, Heimdall is given a moderate hinge offset of 0.10R for low vibrations and small hub drag by providing a virtual hinge through material tailoring.

### 5.2 Blade Root Cutout

Close to the root, the inflow is very low, which has negligible contribution to the helicopter thrust. For this reason, rotor blades aerodynamic surfaces often start beyond the root cutout value which is kept at 0.17R for Heimdall . Elliptical shape sections have been used between the blade grip and the blade root cut out region to minimize the profile drag produced by that region as shown in Fig. 24.

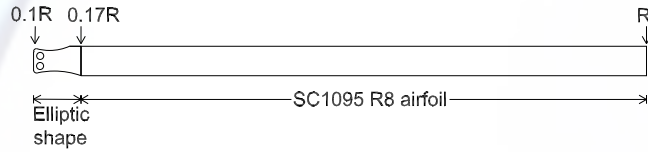


Figure 24: Rotor blade sectional properties

### 5.3 Inter-rotor Spacing

In coaxial helicopters, there is a need to ensure adequate clearance between the upper and lower to avoid the physical contact between the two rotor blades due to the flapping motion. The rotor spacing also influences the performance of the helicopter which is in itself is a major field of research. For Heimdall, rotor spacing ( $h/D$ ) was chosen to be 0.093, based on relative hub clearance data of existing Kamov ka-32 helicopter [11] as Heimdall falls in the same diameter class.

Helicopter	Ka-8	Ka-10	Ka-15	Ka-26	Ka-25	Ka-32	Ka-50
Diameter	5.6 m	6.12 m	9.96 m	13 m	15.74 m	15.8 m	14.5 m
$h/D$	0.098	0.010	0.085	0.090	0.095	0.093	0.097

Table 9: Relative hub clearances of Kamov helicopters [11]

### 5.4 Airfoil Selection

Rotor Performance depends heavily on the aerodynamic characteristics of the blade airfoil sections. Since Heimdall is going to operate at lower forward speeds, reverse flow region on the retreating side is much smaller and retreating blade stall and compressibility effects on blade tip of advancing side are not going to be critical for the current design. Therefore, a single airfoil section is used throughout. It also makes the manufacturing process easy. The major factors influencing the airfoil selection for our helicopter are:

- high lift-to-drag ratio over a wide range of Mach number for better hover performance.
- low aerodynamic pitching moment for lesser control system load.

The former one being the major parameter for the airfoil selection. There are a variety of airfoils available for rotor blade design coming from SC (Sikorsky), RC (NASA), VR (Boeing-Vertol), OA (ONERA) and RAE (Royal Aircraft Establishment) airfoil families. The SC-1095 and SC-1095 R8 were shortlisted for the design because in addition to its readily available aerodynamic characteristics in public domain, these airfoils have proven high performance capability as demonstrated by its use on Sikorsky UH-60 Black Hawk helicopters. Heimdall blade tips are going to operate at around of Mach number 0.4 due to low tip speed. This is well beyond the drag divergence Mach number of both SC 1095 ( $M_{dd} = 0.80$ ) and SC 1095 R8 ( $M_{dd} = 0.78$ ) [12] airfoil.

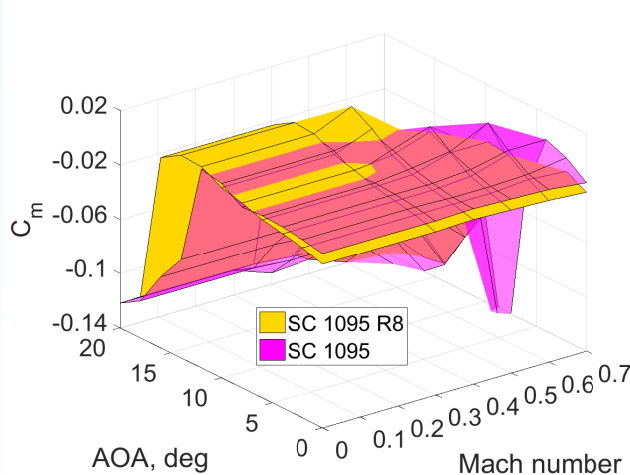


Figure 25: Pitching moment coefficient distribution for SC 1095 and SC 1095 R8

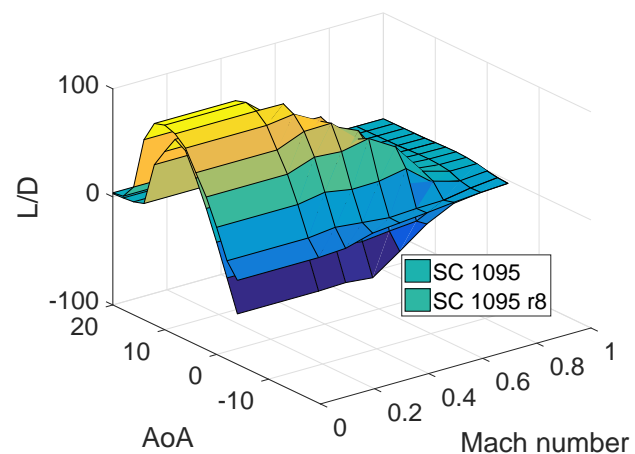


Figure 26: Lift/Drag distribution for SC 1095 and SC 1095 R8

SC 1095 offers slightly lower nose down aerodynamic pitching moment compared to SC 1095 R8 airfoil for all range of Mach number with angle of attack lesser than  $8^\circ$  as shown in Fig. 25. But, SC 1095 R8 airfoil being a thicker airfoil has higher L/D ratio Fig. (26) and also operates at higher maximum lift coefficient for almost all value of Mach number with angle of attack varying from  $0^\circ$  to  $10^\circ$ . Also SC 1095 R8 airfoil has a very high stall angle of attack of around  $16^\circ$ . Keeping in mind, the relative importance of L/D ratio over pitching moment coefficient, SC 1095 R8 airfoil is chosen for the rotor blades of Heimdall .

## 5.5 Blade Twist

Higher blade twist can minimize the induced losses on a coaxial rotor by redistributing the lift over the blade in the hover state however, higher blade twists degrades the performance of the helicopter in forward flight because of the reduced angles of attack on the retreating blade. But since forward flight is not critical for the design, the optimization of blade twist is done only for hovering flight. In the ideal case, hyperbolic and double hyperbolic twist distribution are needed on upper and lower rotor blades, respectively. However, a linear twist distribution is a good approximation [13]. The optimized upper and lower twist are determined using BEMT model. However one limitation of BEMT model is that it doesn't account of the rotor blade stall at high angle of attacks (as airfoil tables have not been incorporated in the analysis). Hence, the angle of attack distribution over the blade was also looked into while changing the blade twists to ensure that at no point of flight the blade goes to stall.

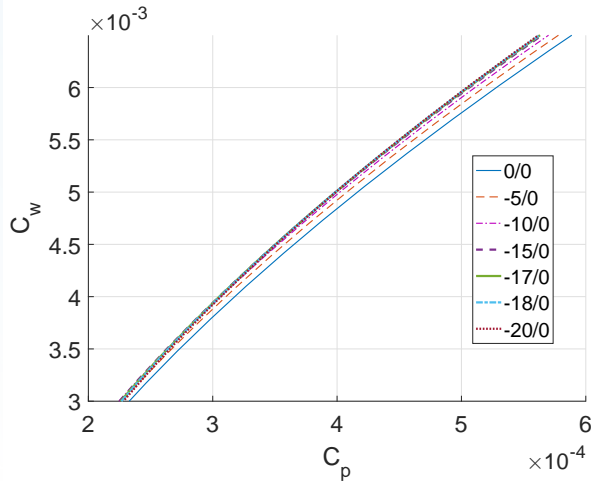


Figure 27: Variation of  $C_T$  vs.  $C_P$  as a function of blade twist rate on upper rotor

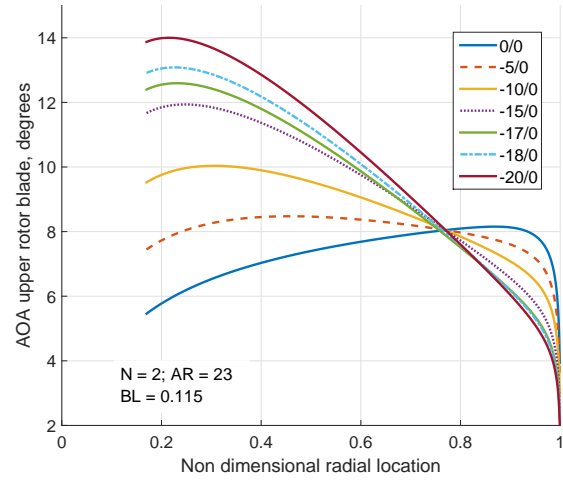


Figure 28: AOA distribution over upper blade during take-off for different blade twist

### 5.5.1 Upper Rotor Blade Twist

In the BEMT analysis, the blade twist of upper rotor is changed from  $0^\circ$  to  $-20^\circ$ , keeping zero twist on the lower rotor blades. The result Fig. 27 showed that with an increase in blade twist of upper rotor, the total power of the combined rotors decreased. Notice that the legend used in the figure denotes the linear twist rate for the upper and the lower rotor blades respectively. But with an increase in the upper rotor blade twist, the upper rotor blade collective required also increased which lead to increased angle of attack inboard on the upper rotor blade and decreased angle of attack outboard. Since SC 1095R8 airfoil stalls at high angle of attack, a twist of  $-18^\circ$  was acceptable as in that case the maximum angle of attack as seen by the upper rotor blade was  $13^\circ$  during take-off as shown in Fig. 28 which is well beyond the stall limit and which eventually decreased with flight time. Therefore, a linear blade twist of  $-18^\circ$  was selected for upper rotor blades.

### 5.5.2 Lower Rotor Blade Twist

Following the determination of upper rotor twist, a corresponding investigation was made to examine the effects of changing blade twist on the lower rotor. In this case, the lower rotor blade twist was changed from  $0^\circ$  to  $-4^\circ$ , keeping the upper rotor blade twist fixed at  $-18^\circ$ . Introducing negative twist rate on the lower blade, increases the angle of attack seen by the blade inboard on the lower rotor but at the same time it also decreases the angle of attack outboard on the lower rotor blade as shown in Fig. 29. Since the inboard region contributes very less as compared to outboard region of the lower rotor blade, the introduction of lower rotor twist rate doesn't improve the rotor performance significantly as seen in Fig. 30. Hence, a small, linear blade twist of  $-3^\circ$  is chosen for the lower rotor blades.

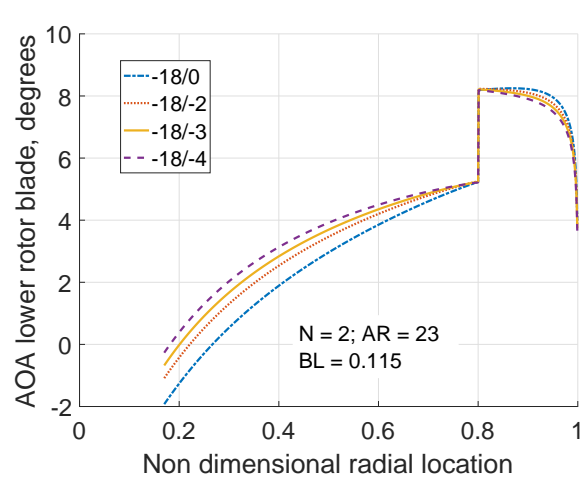


Figure 29: AOA distribution over lower blade during take-off for different blade twist

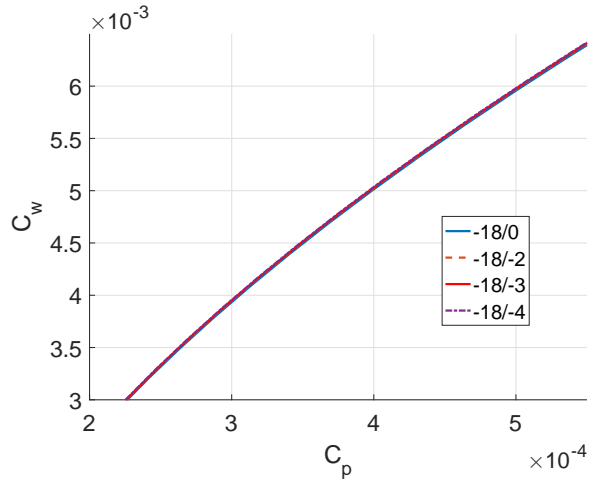


Figure 30: Variation of  $C_T$  vs.  $C_P$  as a function of blade twist rate on lower rotor

The introduction of upper and lower blade twist rate decreases the required power by 4.71% which decreases the fuel weight required to hover for the entire mission time.

## 5.6 Blade Taper

Blade taper is a geometrical means, which optimizes the hovering performance by redistributing the lift over the blade span. However, Heimdall rotor blades have very high aspect ratio and twist and would be complicated to manufacture if taper is also included. Hence, untapered rectangular blades are used in the current design.

## 5.7 Blade Tip Geometry

Blade tip design plays an important role in the performance of the helicopter. Tip sweep decreases the relative speed as seen by the tip of the blade and hence delays the compressibility effect on the rotor blades. Since, Heimdall blade tips operate at very low tip speed, compressibility effect is not significant. Hence, to reduce the blade manufacturing complications and cost, Heimdall has been given simple rectangular tips.

## 5.8 Dissimilar Radius

In coaxial rotor system, the upper rotor radius has a large effect on the overall rotor system as it not only affects the upper rotor but also the lower rotor which operates under the influence of lower rotor. A recent study proposed the use of dissimilar rotor radii for coaxial rotor system for power reduction [14]. This approach is incorporated in current design approach to further optimize power. For this, the radii of the rotors are varied such that equivalent rotor area is maintained. A design variable,  $a$  was used for denoting both the radii. Using this variable, the upper and lower rotor radius are defined as:

$$R_{(u)} = aR_{BL}$$

$$R_{(l)} = R_{BL}\sqrt{2 - a^2}$$

where  $R_{BL}$  is the baseline radius. The rotors radii are changed keeping the aspect ratio of both upper and lower rotor blades constant at 23. Hence, with changing radii, the chord length of both the rotors will also change. With this, manual optimization is done by comparing thrust versus power coefficients using the BEMT model. Since both the rotors have different radii, thrust and power coefficients are defined as thrust and power non-dimensionalized using the baseline radius.

$$C_T = \frac{T}{\rho \pi R_{BL}^2 (\Omega R_{BL})^2}, C_P = \frac{P}{\rho \pi R_{BL}^2 (\Omega R_{BL})^3}$$

From Fig. 31 we can see that as  $a$  decreases below 1 i.e., the upper rotor radius is decreased and lower rotor radius is increased, the power required to hover decreases for the same weight of the helicopter. This is because as we decrease the upper rotor radius the area of lower rotor under the wake of upper rotor decreases Fig. 33 due to which the induced power of the inboard section of the lower rotor decreases and eventually thrust and power sharing of both the rotors become equivalent. Also, due to reduction of upper rotor radius, the upper rotor blade now operates at higher collective pitch which reduces the stall margin of the upper rotor blade.

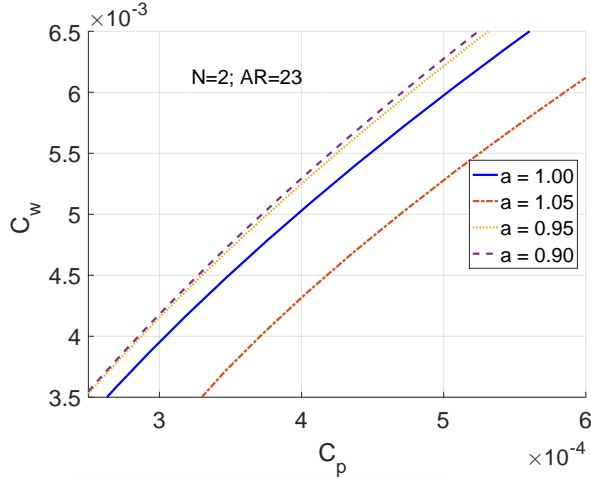


Figure 31: Variation of  $C_T$  vs.  $C_P$  for different values of dissimilar radius factor

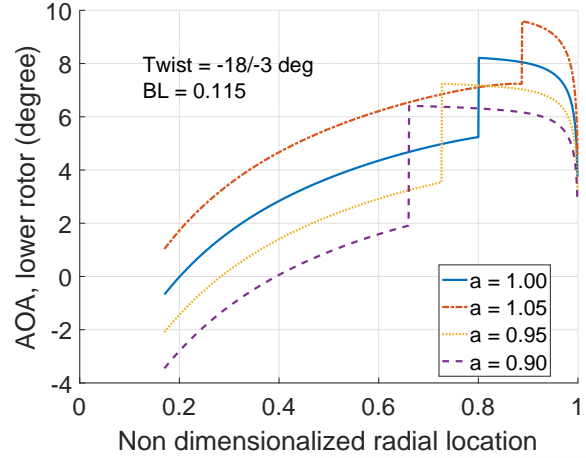


Figure 32: AOA distribution over lower blade during take-off for dissimilar radius optimization

For the optimization,  $a = 0.95$  was chosen, as in this case the upper rotor operates at maximum angle of attack of  $14.7^\circ$  at non-dimensional radial location of 0.25 as shown in Fig. 33 during take-off. The section at nondimensionalized radial location of 0.25 operates at Mach number which is equal to  $0.25M_{Tip}$ , which is around 0.1. At this Mach number the SC1095 R8 airfoils stall at  $16^\circ$  angle of attack. Hence angle of attack of  $14.7^\circ$  is acceptable. For lower values of  $a$  the upper rotor goes into stall.

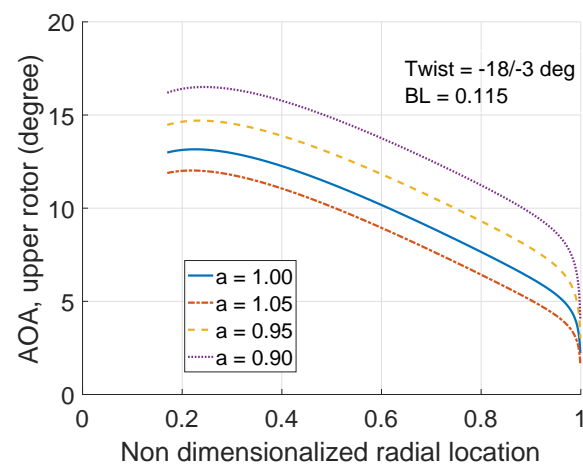


Figure 33: AOA distribution over upper blade during take-off for dissimilar radius optimization

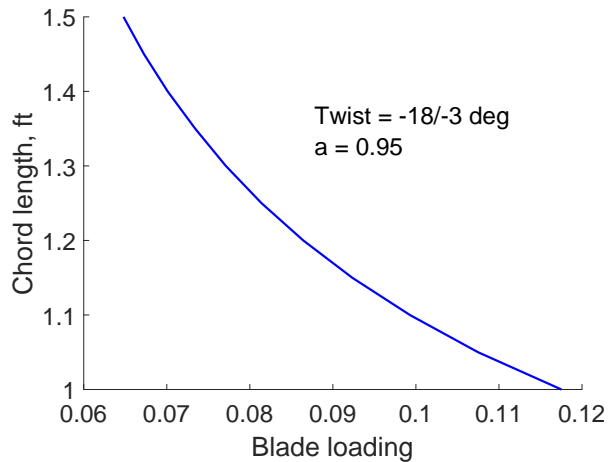


Figure 34: Blade loading versus chord distribution for the optimized design

The use of dissimilar radius further decreases the required power by 5.5%. Again, weight analysis is repeated as discussed in section 3.7, to get the optimized results for Heimdall which is discussed in the next section.

## 5.9 Optimized Results for Heimdall

This section discusses the final parameters for Heimdall after the aerodynamic optimization. As power required decreases due to optimization of the rotor system, the required fuel weight decreased and hence the gross weight, which eventually caused the blade loading at take-off to go lesser than 0.115. But as discussed in the preliminary sizing section, we intend on keeping our blade loading at take-off to be 0.115, which is achieved by decreasing the baseline chord length of the rotor blades to 1.01 ft as shown in Fig. 34. This also results in a decrease in the empty weight. Weight analysis (done similarly as in section 3.7) after this optimization, keeping the design variables fixed ( $N_b = 2$ ,  $AR = 23$ , Blade Loading = 0.115 and  $V_{tip} = 450\text{ft/s}$ ) gave us the following result:

1. Baseline chord = 1.01 ft
2. Baseline radius = 23.23 ft
3. RPM = 184
4. GTOW = 5195 lb (2356 kg)
5. Fuel weight = 2360 lb (1070 kg)
6. Empty weight fraction = 0.5116
7. Take-off power = 400 hp
8. Rotor spacing = 4.32 ft

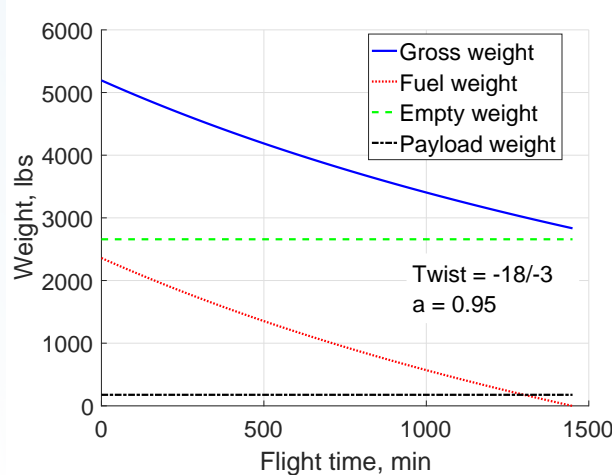


Figure 35: Variation of Weight with hovering time for the optimized design

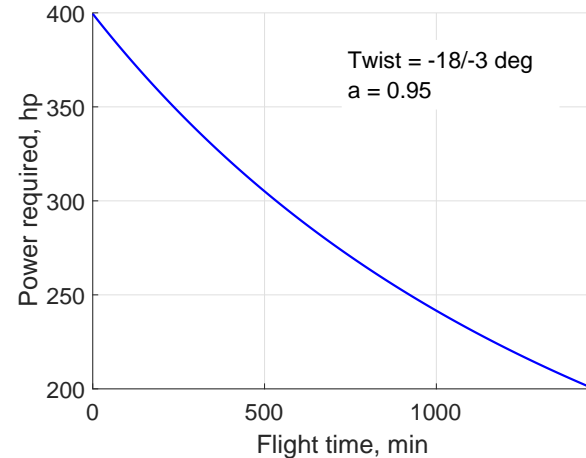


Figure 36: Variation of required power with hovering time for the optimized design

The gross take-off weight of Heimdall is 5195 lbs, which carries fuel of 2357 lbs. The key parameters of the optimized coaxial rotor system designed are listed in Table 10. The final dimensions of the vehicle are shown along with their drawings in foldout-1. With time the fuel gets consumed and gross weight decreases and at the end of 24 hours and 10 minutes the fuel weight goes to zero (see Fig. 35). As the weight goes down with time, so does the power required from 400 hp to 200 hp at the end of the flight as shown in Fig. 36.

	Upper Rotor	Lower Rotor
Aspect Ratio	23	23
No. of Blades	2	2
Blade Chord	0.3 m (0.96 ft)	0.323 m (1.06 ft)
Radius	6.727 m (22.07 ft)	7.42 (24.34 ft)
Tip speed	130.3 m/s (427.5 ft/s)	143.7 m/s (471.5 ft/s)
Blade twist rate	-18°	-3°
Hinge offset	0.1R	0.1R
Root cutout	0.17R	0.17R

Table 10: Rotor optimized design parameters

As demanded by the RFP, the variation of figure of merit of Heimdall with the blade loading is shown in Fig. 37. From the figure we can see that Heimdall offers an excellent figure of merit of 85% during take-off which proves our claim of Heimdall being the most efficient hovering machine. At higher blade loading the figure of merit is expected to decrease due to stall.

We know that figure of merit is defined as

$$FM = \frac{P_{ideal}}{P_{meas}}$$

$$P_{ideal} = \frac{T_u^{1.5}}{\sqrt{2\rho A_u}} + \frac{T_l^{1.5}}{\sqrt{2\rho A_l}}$$

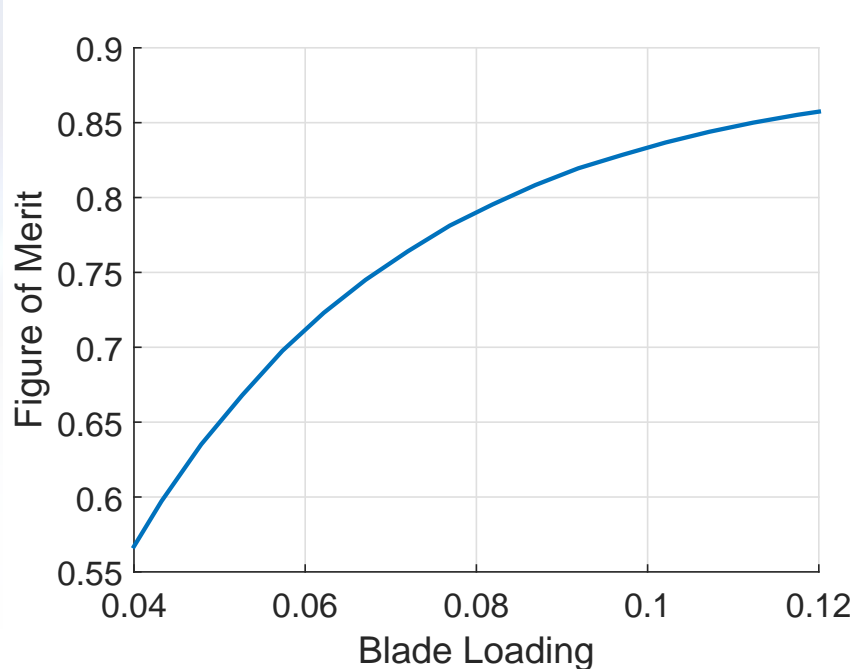


Figure 37: Variation of figure of merit with the blade loading

Here,  $P_{meas}$ ,  $T_u$  and  $T_l$  are the actual measured power, upper rotor thrust and lower rotor thrust, respectively. All these values are estimated using the BEMT analysis.

## 5.10 Rotor Blade Structural Design

Carbon reinforced composites are used extensively in the construction of the rotor hub and blades of the Heimdall . Their high strength and stiffness characteristics allow the blades to be lighter, while their high damage tolerance, superior fatigue properties, and their soft failure modes increase structural integrity and safety. In addition to this, composites offer greater resistance to corrosion, less demanding to repair and have a fatigue-life of up to five times longer than comparable aluminium alloy blades.

### 5.10.1 Material Selection

Unidirectional fiberglass, carbon fabric, rohacell foam and chopped strands of carbon fabric were considered for blade construction materials. Fiberglass offers affordability and transparency to radar, but doesn't offer the specific strength or specific stiffness of carbon fabric. Carbon fabric is chosen because of its superior stiffness and strength characteristics, allowing for weight savings in both the hub and rotor blades. Rohacell foam is considered for the core of the rotor blades on which the fabric layers can be laid. The advantages of this foam is, it has excellent dynamic strength, light weight material and can be easily machined into desired shapes. The specific composite materials used for the rotor blade construction and their mechanical properties are listed in Table 11 [16].

Material	Density ( $gm/cm^3$ )	Young's Modulus (GPa)	Fibre Tensile Strength (GPa)
Fiberglass	2.55	72	3.4
Carbon Fabric	1.65	275-345	4.8
Rohacell	0.032	0.036	0.001

Table 11: *Properties of materials used in the blade manufacturing*

### 5.10.2 D-Spar

Several blade spar configurations were considered to determine the optimum solution to support the blade structure. After evaluation, two candidates (C-spar and D-spar) were shortlisted, and their structural properties were further investigated. D-spar design offers a simple, closed-section structure with high torsional rigidity. IC-spar design, with a primary spar near the leading edge and a second spar near the mid-chord, allows easy positioning of centre of gravity without a non-structural nose weight. Although a small weight reduction can be realized with the C-spar design, it was not chosen since it requires higher manufacturing labour due to two spars. Therefore, a D-spar configuration is chosen for the Heimdall .

### 5.10.3 Blade construction

The blade spar is constructed of unidirectional fiberglass providing high tensile strength while minimizing material cost. The outer blade skin consists of carbon fabric and unidirectional fiberglass to provide high bending stiffness and minimize weight. Rohacell foam is selected as the core material due to its advantages mentioned in above section (see section 5.10.1). A tungsten mass ballast weight is used in the nose of the blade to bring the centre of gravity marginally ahead of quarter-chord, which is required to ensure aeroelastic stability of the blades. The D-spar is constructed with 18 layers of unidirectional fiberglass with rohacell foam as the core. The D-spar will be formed as a separate part and later laid up with the rest of the blade structure. The trailing edge is made of chopped carbon fibre strands mixed with epoxy. This was done to make the trailing edge rigid and to make it easily machinable. The outer blade skin consists of one layer of unidirectional fiberglass and 8 layers of carbon fabric. Erosion of the rotor blade leading edges due to collision with water, particles, sand and debris is an important consideration. This will reduce the aerodynamic performance as result of flow separation. So, the front half of the blade is covered with sheet made up of steel. The detailed description of the blade cross-section is shown in (fold-out ref).

## 5.11 Hub Design

To design the hub of Heimdall we gave priority on mechanical simplicity, reduced cost of manufacture and reduced maintenance. In a fully articulated rotor system, each rotor blade is attached to the rotor hub through a series of hinges that let the blade move independently of the others. In a rigid rotor system, each blade flaps and drags about flexible sections of the root. Therefore, upon comparing the above two rotor hub systems we can easily see that rigid rotor system is mechanically simpler than a fully articulated rotor system. Besides, loads from flapping and lead/lag forces are accommodated through rotor blades flexing, rather than through hinges which results in the blades compensating themselves for the forces that previously required rugged hinges. This creates less lag in control response because of the large hub moment typically generated. Elastomeric bearings are used in

place of conventional roller bearings. Such bearings are constructed from a rubber type material and provide limited movement that is perfectly suited for helicopter applications. Besides, they require no lubrication and, therefore, require less maintenance. They also absorb vibration, which means less fatigue and longer service life for the helicopter components. The lead-lag motion is also damped using elastomeric damper. Also flex beams are used in the hingeless hub to reduce the complexity and the weight of the rotor hub.

## 6 Drive Train

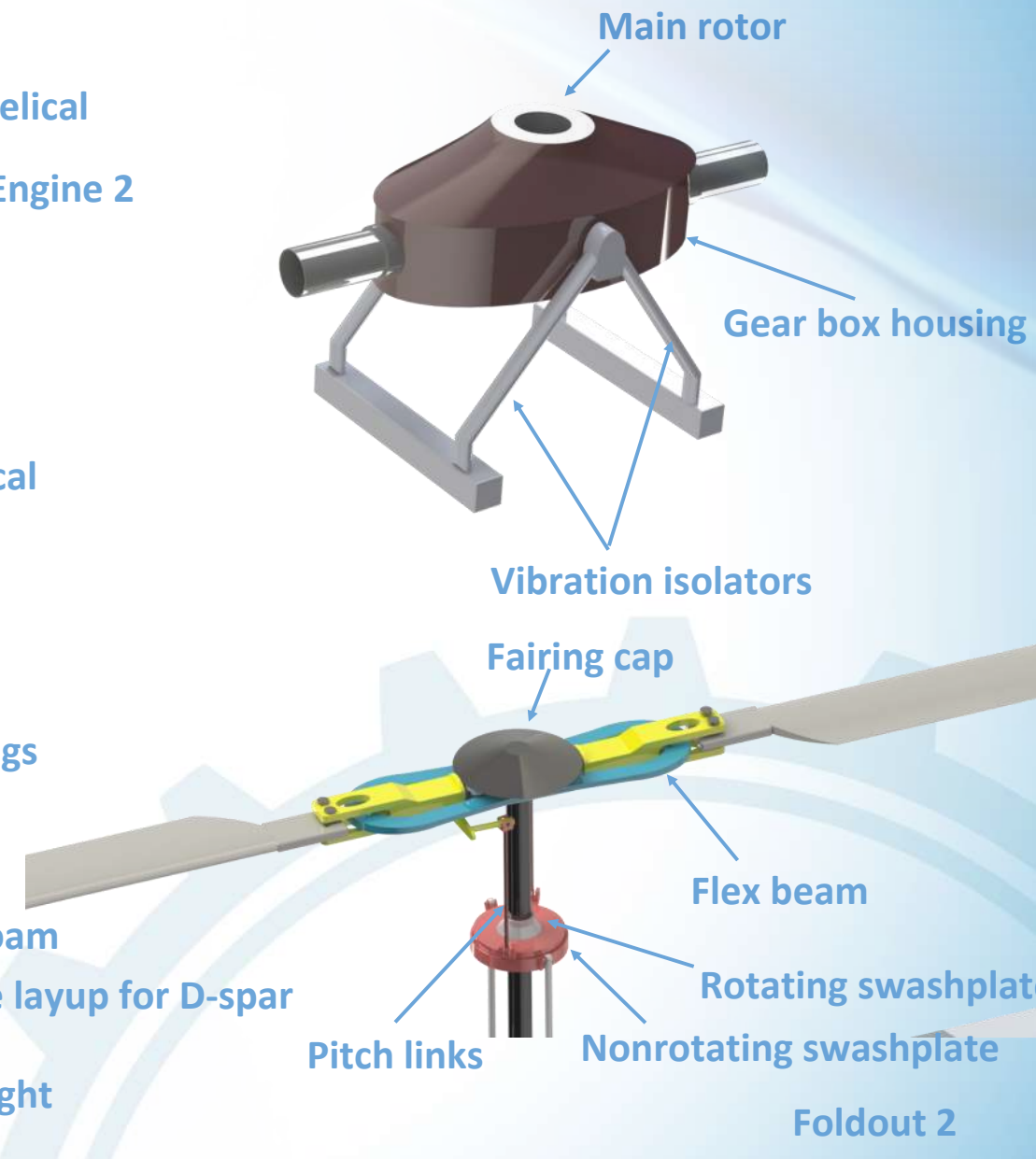
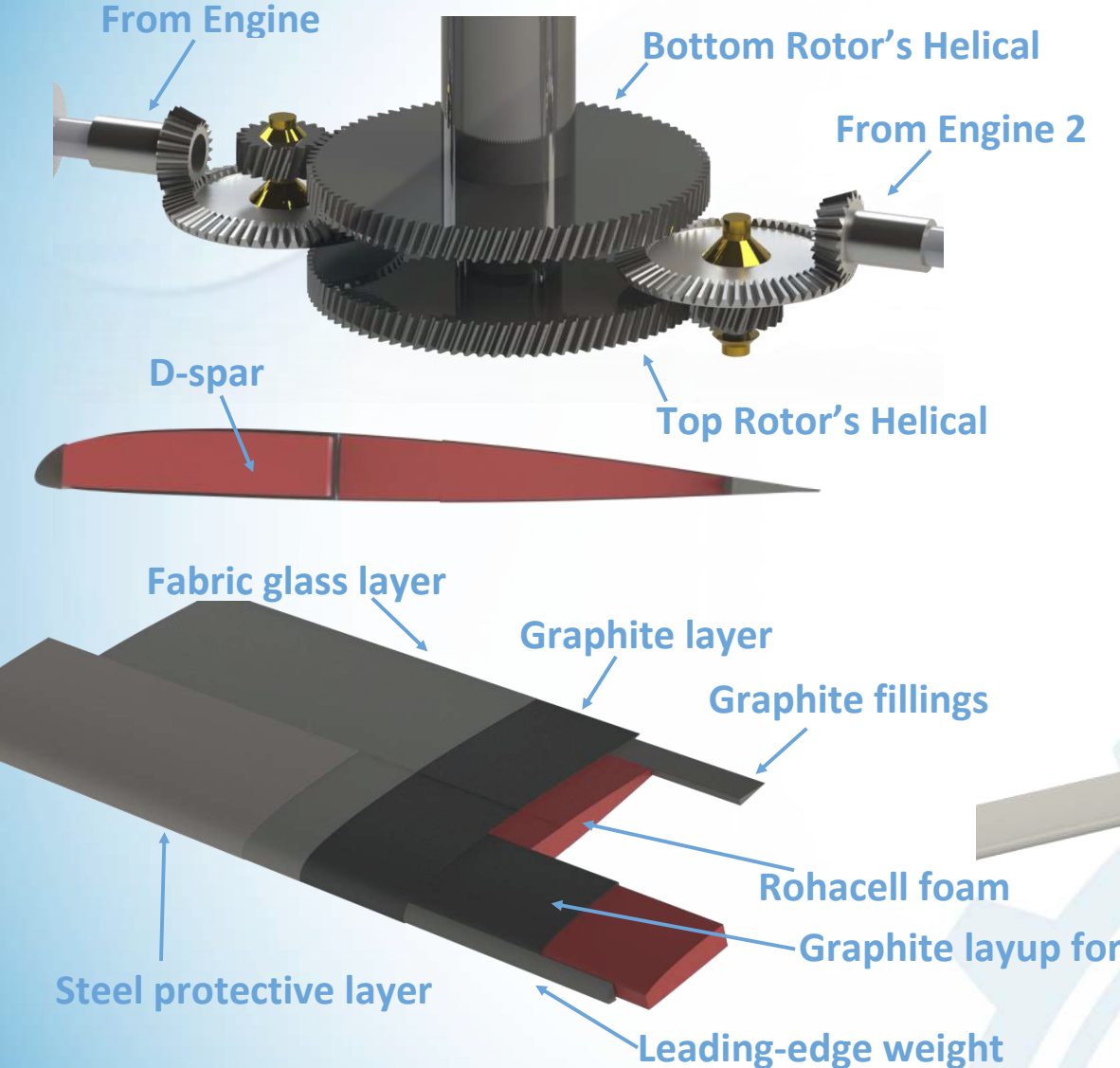
The aim of this section is to design and model a transmission system that would take input from the two aircraft engines and distribute power to the two rotors. Both the upper and lower rotors are designed to operate at same rotational speeds throughout the mission but having different direction of rotations. As per the RFP, the Heimdall has to only hover for most part of the mission hence hovering endurance is a critical parameter. Because of the need of high hover endurance, the download on the fuselage should be reduced hence the major consideration while designing the transmission system was to minimize gearbox weight while maximizing compactness. The others parameters that were considered in design process of the transmission system are overall simplicity, ease of assembly/disassembly, vibration minimization and manufacturability issues.

### 6.1 Transmission system configuration

From the previous section 5.9 it is established that the two main rotors are going to operate at 184 RPM. The drive train is powered by two zache-O2A engines. The standard dimensions of this radial engine are 65 centimetres diameter and 84 centimetres length. The engines drive the system with an input speed of 2500 RPM [15].

Knowing the RPM output of the engine and RPM input required to rotate the rotor shaft, the total reduction ratio was calculated to be 13.8. This reduction in the RPM was achieved in two stages. The foldout-2 shows the layout and gives relevant information about the engine and the transmission system. In the transmission system of Heimdall , each engine has been individually connected to each of the two main rotors. The main reason for the selection of this configuration was to maximize the compactness. If both the engines are coupled beforehand of the transfer of power to the main rotors, then the engines had to be mounted side-by-side, which would have increased the width of the fuselage and also would have displaced the centre-of-gravity to the side where they would have been mounted. This would have increased the stress at the point of transfer of power to the two main rotors. So in the final design of transmission system, one engine is mounted ahead of main rotor hub and other is mounted at the back of main rotor hub. Also the rotor output shafts lie on the line passing the length of the fuselage. With both of these considerations in mind it was decided to run the engines output shaft into a straight bevel input pinion gear that meshes with a straight bevel gear. The specifications of all the gears are given in Table 12.

# Transmission and Rotor System



Stage	Stage 1	Stage 2
No. of teeth (pinion/gear)	20/60	20/92
Reduction ratio	3	4.6
Module	3	3
RPM (pinion/gear)	2500/833.33	833.33/184
Face width (mm)	24	25

Table 12: *Transmission gear specifications*

In stage 1, there is a reduction of 3. Then the torque is transferred to the helical input pinion gear, which meshes with a helical gear that is connected to one of the main rotors shaft. At this point, there is a reduction of 4.6. Same drive train is designed for the other main rotor also. The gear sizing is done based on [17]. Nickel chromium steel alloy are considered as material for the transmission system due to its high hardness and good wear resistance. And also nickel chromium alloys are also economical. The total weight of the transmission system is estimated to be 225 lbs.

## 7 Airframe Design

The structural layout of Heimdall consists of three sections: cockpit, central fuselage and tail section. Cross-section of the fuselage varies with fuselage length to improve the aerodynamic and structural characteristics. The cockpit carries a payload represented by an human body and all the avionics and control systems. The central fuselage consists of two cabins separated by deck for mounting engines and transmission system. The upper cabin consists of two engines that are placed opposite to each other with the transmission system at the centre. We decided to insert transmission and power plant in the central fuselage, because the mission gives us the freedom of using cabin space for helicopter subsystems, since we don't have to carry passengers or large amount of cargo. The lower cabin of the central fuselage includes fuel tanks, and avionics. Thus, making the available space optimum for the required subsystems.

The dimensions of the fuselage are decided considering the space required to install two diesel engines around the transmission systems and payload represented by human.

### 7.1 Structural Details

The Airframe structure consists of five lightweight primary bulkheads which serve to connect three sections, bear the loads and bending moments. Two keel beams are placed along the length of the fuselage and are designed in such a way so as to absorb energy upon impact. Additional beams running along the length of the transmission deck serve to provide load paths for the diffusion of rotor loads. The first primary bulkhead was present in the cockpit and supports the avionics and payload. The second primary bulkhead was at the start of central fuselage. It is also the front support to transmission deck. Central support to transmission deck is offered by third and fourth primary bulkheads. They were equally spaced along the length of the central fuselage. They also supports the landing gear. The fifth primary bulkhead is the aft of the transmission deck. There are two secondary bulkheads at the nose of the fuselage and at the point that connects the central fuselage to tail boom. There are also many thin stringers that were included in the airframe in order to reduce the load on bulkheads and maintain the shape of the skin. The cross-section of the cabin is a bit ellipse in

shape. The ellipse shape of the fuselage was to reduce the download on the fuselage due to the rotor downwash. The whole airframe structure is shown in foldout-3.

### **7.1.1 Transmission and Powerplant Deck**

The Transmission deck provides structural support to two engines and transmission system along with the auxiliary power units, electric systems and hydraulics. The whole drive train was kept inside the housing. It was shown clearly in foldout(ref). All the subsystems above the transmission deck were covered with cowl which was supported by stringers. The top part of transmission system housing was covered with rotor pylon fairing.

### **7.1.2 Fuel Tank**

Apart from positioning of transmission and power plant, special care was taken for the placement of fuel tank system and payload. The Fuel system has relatively more contribution to the gross weight, carrying approximately 40% of the gross weight of the Heimdall . During a 24hr hover mission, CG travel needs more attention. The total fuel required for the mission was distributed in to three tanks and placed in a way that the center of gravity of the whole fuel system remains almost fixed.

## **7.2 Crashworthiness**

Our design focus on materials used in airframe always revolved around composite structures considering energy management during crash.

The main advantage of composite materials over conventional isotropic materials are the very high specific strengths and specific stiffness which can be achieved. Besides the perspective of reduced weight, design flexibility and low fabrication costs, composite material offer a considerable potential for light weight energy absorbing structures. We have considered two primary design goals for crashworthiness, they are to restrict the impact forces transmitted to the payload and to maintain the structural integrity of the fuselage. Therefore, the airframe is designed with resilience to protect its payload. Some of the failures in our mission may cause events like Obstacle strike, Rollover or Ground crash. Throughout the airframe, structural members have been sized and placed so as to keep the structure intact during crash events. The frame of keel beams is designed and mounted to absorb energy by collapsing in a high buckling mode. The bulkheads and stringers are arranged to dissipate energy so that the loads are substantially reduced before reaching our interior of fuselage. During the ground strike events, the high torsion and bending moments can cause the transmission to enter the lower cabin, making the lower cabin more dangerous. So, we decided to place our payload in the cockpit area separated by a surface supported by a bulkhead.

## **7.3 Material selection**

In Heimdall ,composites were mostly considered to reduce the structural weight as much as possible. Other than composites, metal alloys like aluminum-lithium alloys, Ni-Cr steel were also considered for higher strength and low density. The bulkheads, stringers and keel beams of the airframe were of composites. The gears of the transmission system were up of Ni-Cr steel and the gearbox housing was of graphite/ glass fibre/ epoxy skin. The airframe skin and rotor hubs were also of the composites. The engine deck is made of titanium alloy plate with honeycomb structure for its high resistance to

heat and fire, as well as oil corrosion. Aluminum alloys were considered for the skid landing gear of Heimdall .

## 7.4 V-Nz plot

The load factor versus velocity diagram for the Heimdall structural limiting load envelope is constructed for a rotorcraft designed for a limit maneuvering load factor ranging from a positive limit of 2.0 to a negative limit of -0.5. The requirements was reduced to smaller range of positive 2.0 to negative 0.5 due to the benign mission requirement of continuous hover and low forward speed. The critical air-speeds of the Heimdall are calculated according to the reference [18]. The limits at high airspeed are determined by rotor blade stall and blade tip Mach number limits. The maximum level flight speed for Heimdall  $V_H$ , in forward flight is 204 knots using the performance analysis of the design discussed later. The design limit speed,  $V_{DL}$ , is calculated using a factor of 1.15 times  $V_H$ , a typical ratio for surveillance helicopters, which comes out to be 234.60 knots. The never exceed speed,  $V_{NE}$ , is assumed to be equal to  $V_{DL}$  for preliminary design purpose.

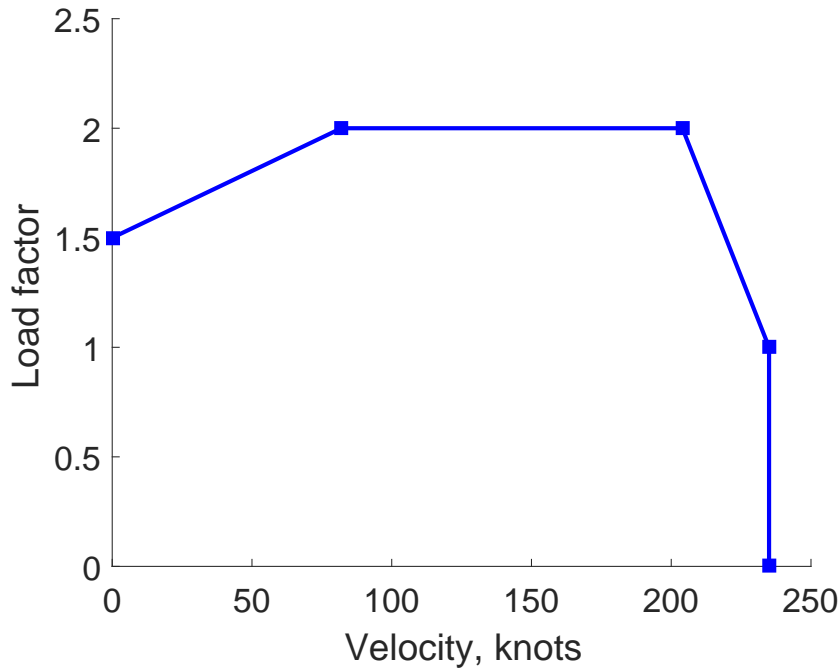


Figure 38: V-Nz plot for Heimdall

## 8 Landing Gear Design

The landing gear supports the entire weight during landing and ground handling of the helicopter. It absorbs the vertical energy which is produced due to the landing impact and also provide a resilient and stable suspension with the added capability to avoid ground resonance.

## 8.1 Landing Gear Classification

Helicopter landing gear configurations mainly include skid or wheel type system (fixed or retractable). Skid gears have been used for low gross weight helicopters for many years. As the gross weight increases, tricycle tailwheel or nosewheel types have been used.

### 8.1.1 Skid vs Wheel Type Landing Gear

Skid landing gear systems are mechanically very simple to design, lighter in weight, easier to maintain and less costly than wheel type landing gears. However, they produce higher parasitic drag in forward flight and may suffer from ground resonance.

## 8.2 Landing Gear Selection

Since our mission mainly consists of hovering flight at sea level, the critical parameter for the landing gear design was the weight of the system. Hence for the Heimdall , a non-retractable skid type landing gear system is selected. Typical skid landing gear consists of forward and rear cross tubes and two skid tubes. Replaceable wear plates are provided at the bottom of the skid tubes to prevent damage to the load bearing tubes. The deflection of cross tubes plays the role of a shock absorber during landing operations.

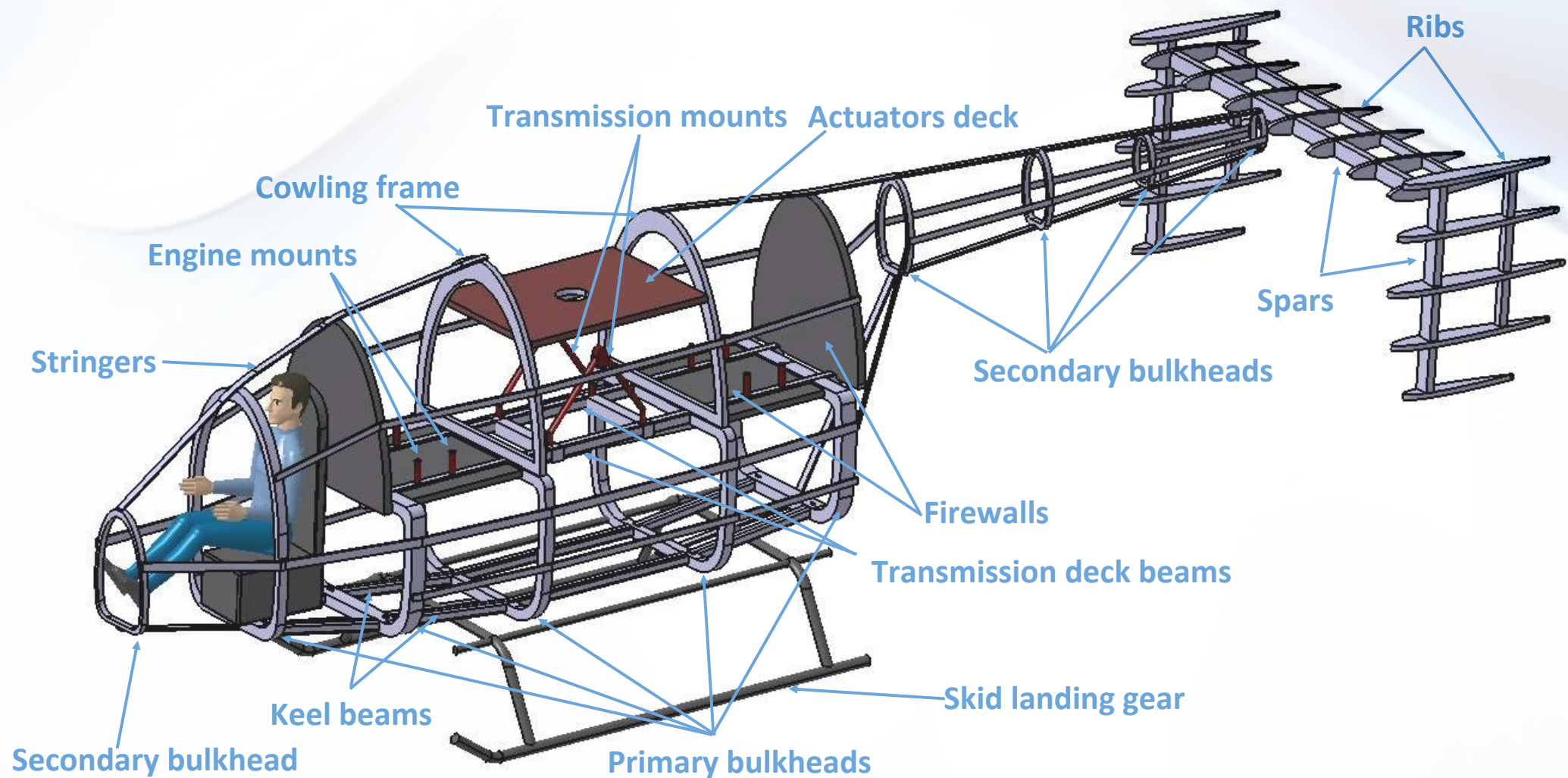
### 8.2.1 Retractable vs Non-retractable Landing Gear

Retractable landing gear systems have drastically higher weight and lesser crashworthiness than the non-retractable landing gear system. However they enhance the forward flight performance of the helicopter by eliminating the parasite drag contribution of the landing gear.

## 8.3 Static Stability Angle Analysis

The pitch and roll static stability angles are defined as the position of the ground contact points in relation to the centre of gravity of the helicopter. The roll stability angle must be less than  $60^\circ$  and the pitch stability angle must be less than  $30^\circ$  to ensure lateral static stability and longitudinal static stability, respectively. Heimdall 's landing gear has been designed to ensure pitch and roll static stability by keeping the roll stability angle lesser than  $60^\circ$  and pitch stability angle lesser than  $30^\circ$ .

# Heimdall Structural Layout



## 8.4 Structure Analysis

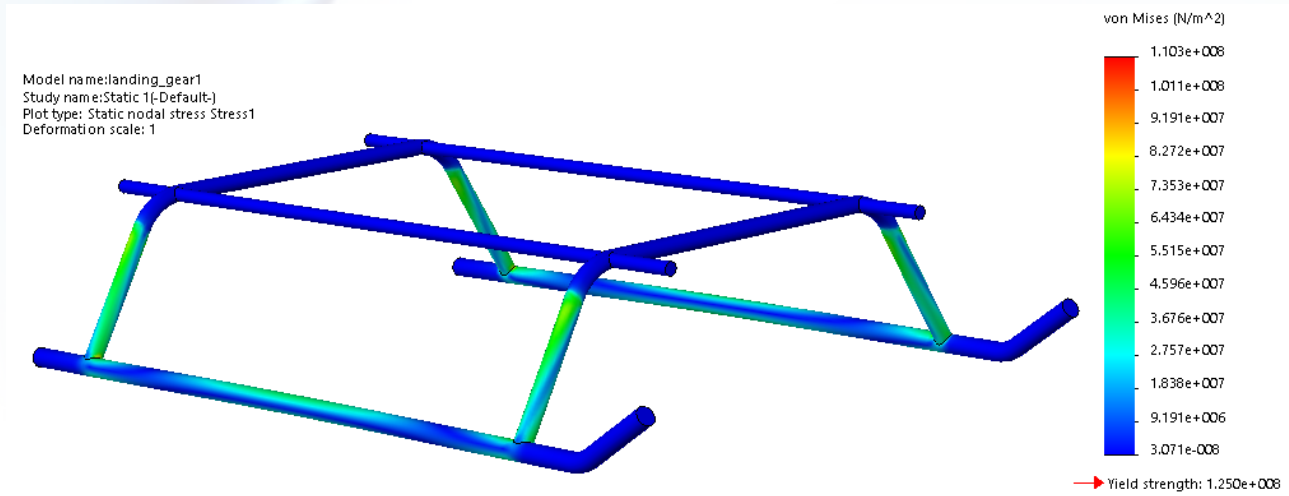


Figure 39: Stress Plot on the landing gear

A static stress analysis was performed on the landing gear of Heimdall using FFEPlus solver of Solidworks. The material for the landing gear used for the analysis was Aluminum 1060 H-18 alloy with Linear Elastic Isotropic Model Type. A geometrical fixture was applied to the upper 4 rods and a force equivalent to half of the gross take-off weight of the Heimdall was applied to both the lower skid rods. The minimum and maximum von Mises Stress came out to be  $3.071e - 8N/m^2$  and  $1.103e + 8N/m^2$  respectively. As the yield stress is  $1.250e + 8N/m^2$  no failure occurred during the structural simulation of the landing gear. The stress plot of the landing gear is given in Figure 39.

## 9 Drag Estimation

### 9.1 Parasitic Drag

The parasitic drag estimation for the current design is done according to Prouty's method [6]. The frontal flat plate areas for individual components are given in Table 13. These are calculated from the drawings and combined with factors given by Prouty. A factor of 20% has been added to the total as recommended by Prouty for more realistic results. The fuselage of Heimdall is designed to be compact and streamlined. However, the relatively low maximum cruise speed requirement made aerodynamic cleanliness less critical. While the landing gear is skid type, it is a source of drag in forward flight.

### 9.2 Vertical Drag

Vertical drag penalty in hover for Heimdall was estimated according to the method proposed by Prouty[6]. This method estimates the drag on whole fuselage by partitioning the fuselage into several sections. The dynamic pressure was also considered varying along the blade radius. The vertical projected area of each section was calculated for calculating the drag on that section. The total projected area of the fuselage was calculated using drawings.

<b>Component</b>	<b>Horizontal <math>C_D</math></b>	<b>Flat Plate Area (<math>m^2</math>)</b>	<b>Flat Plate Area (<math>ft^2</math>)</b>
Fuselage	0.06	0.465	5.01
Rotor hub & Shaft	1.06	0.562	6.05
Landing gear	1.01	0.09	1.05
Horizontal stabilizer	0.021	0.019	0.208
Vertical stabilizer	0.013	0.017	0.189
Rotor-Fuselage interference		0.12	1.3
Exhaust drag		0.046	0.5
Miscellaneous drag		0.046	0.5
Subtotal		1.37	14.8
20% Growth		0.27	2.96
<b>Total flat plate area</b>		<b>1.65</b>	<b>17.77</b>

Table 13: *Component drag breakdown*

The total projected area was found out be  $53.49 \text{ ft}^2$ . From this the ratio of vertical drag to gross weight was equal to 0.031. And the ratio of vertical projected area to the area of the rotor disc was equal to 0.09.

## 10 Forward Flight

A trim model of coaxial helicopter using Newton Raphson approach, as described in [19] is utilized to analyse the coaxial rotor dynamics in forward flight of the helicopter. The blades were modelled as rigid blades with hinge offset and root spring with only flap degree of freedom. Aerodynamic loads are estimated using Blade Element Theory (BET) coupled to Drees inflow model. The power requirements in forward flight are calculated after trimming the helicopter at each speed, taking into account the drag due to the angle of attack of the fuselage and the rotor blades. The complete algorithm is described in the flowchart depicted by the Fig. 40.

### 10.1 Performance Analysis

At the end of the iteration we get the blade control angles and power vs speed graphs as shown in Figs. 41 and 42. The attitude attained by the helicopter during trim is shown in Fig. 43.

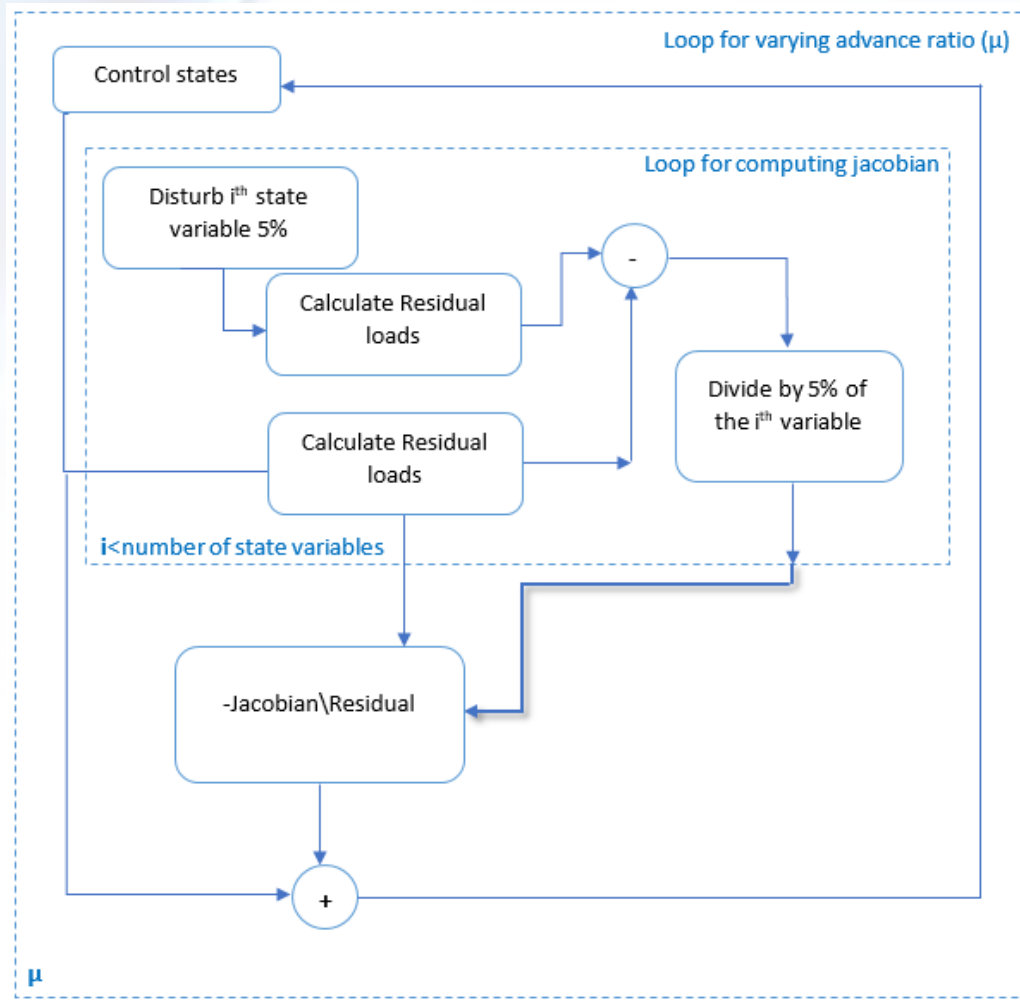


Figure 40: Trim algorithm for forward flight performance prediction

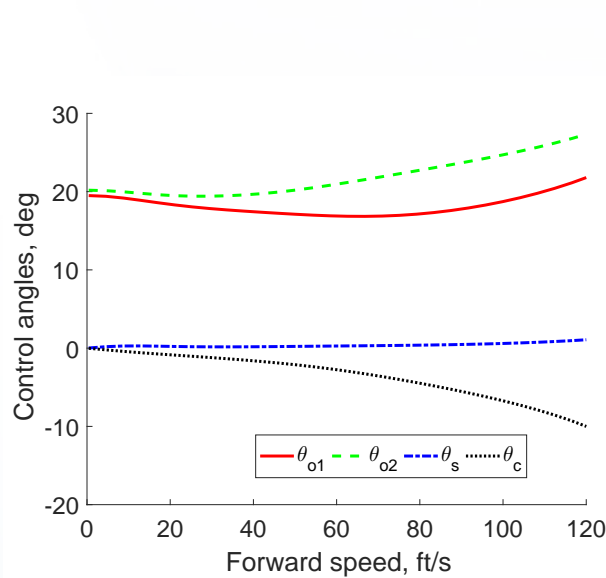


Figure 41: Control Angles at different forward speeds

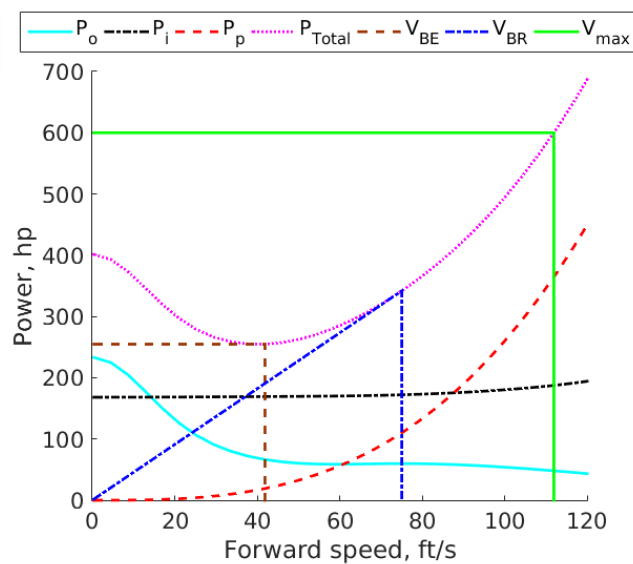


Figure 42: Power required at different forward speeds

The points for maximum endurance and maximum range of the helicopter are marked by brown and blue dashed lines and it corresponds to 42 ft/s (25 knot) for best endurance, and 75 ft/s (44.5 knot) for best range. Since, we know the net power available (from engine) we can also get the maximum speed at which the helicopter can fly which is 112 ft/s (67 knot), marked by the green line. As expected the forward flight performance is inferior to a typical helicopter, as the hover performance has been the primary design driver. Also, shown in Figs. 44, 45 and 46 are the variation of endurance, range and maximum climb rate as function of forward speed. Therefore, the performance analysis enables us to establish the performance capabilities of Heimdall . The design boasts of hover endurance of 24 hours which increases to 35 hours at best endurance speed. It also has a maximum range of nearly 1438 miles at best range speed mentioned above.

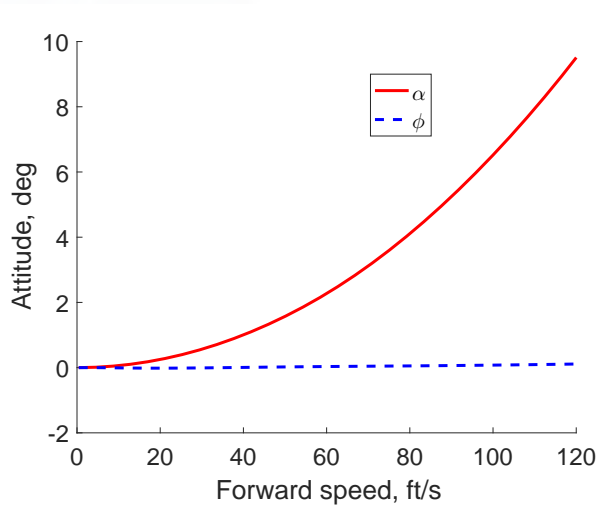


Figure 43: Attitude at different forward speeds

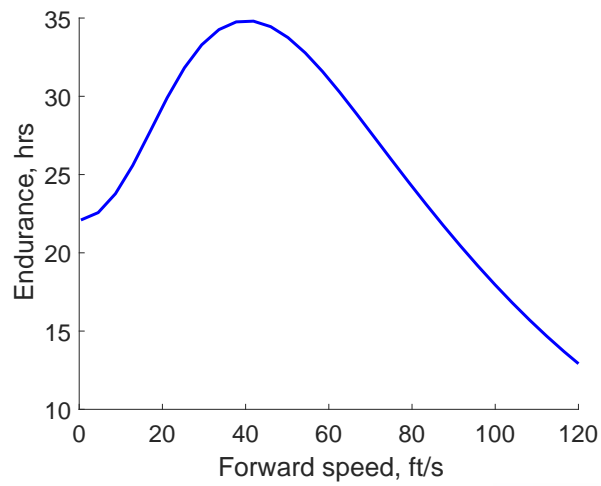


Figure 44: Endurance at different forward speeds

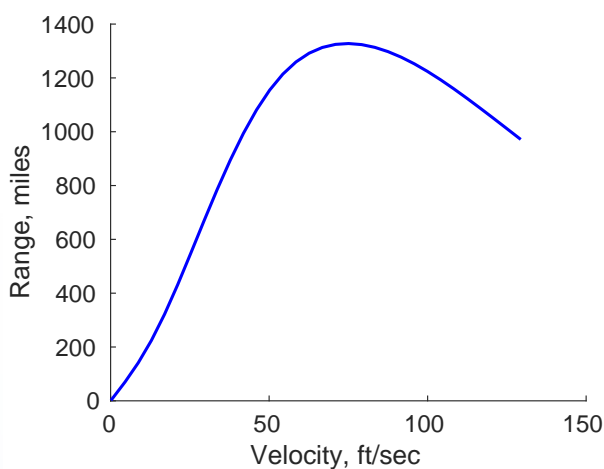


Figure 45: Range at different forward speeds

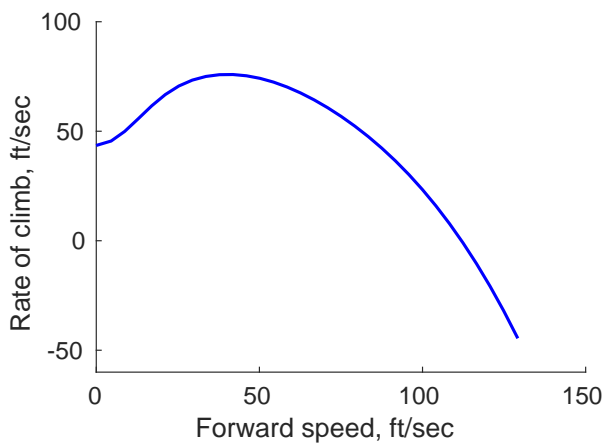


Figure 46: Rate of Climb at different forward speeds

# 11 Stability Analysis

## 11.1 Lateral and Longitudinal Modes

A simplified linear flight dynamic model is developed based on the method described by Padfield in which the helicopter loads are calculated through numerical integration and perturbed numerically to find out the stability and control derivatives about the trim condition for hover flight. The linear model was used with stability derivatives at each trim point as in the following equation:  $AX = Bu$ , where  $X$  is the state vector,  $u$  is the control input,  $A$  is the stability matrix, and  $B$  is the control matrix.

For hovering flight of Heimdall the matrix  $A$  is determined and used to compute the eigen values representing the various modes of the helicopter. These eigenvalues are plotted and shown in Figs. 47 and 48. The numerical values of all the eigenvalues are displayed in Table 14. There are three oscillatory modes and two stable modes for the eigenvalues in hover state.

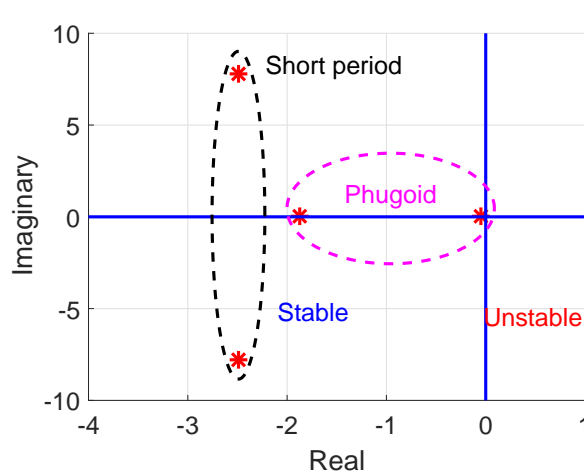


Figure 47: Eigen value plot for Longitudinal Hover Stability

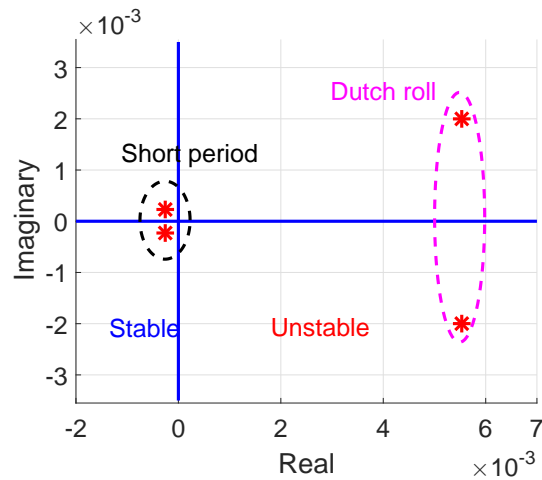


Figure 48: Eigen value plot for Lateral Hover Stability

Eigenvalue	Type
-2.485 + 7.791i	Phugoid
-2.485 - 7.791i	Phugoid
-1.870	Roll mode
-0.043	Spiral
0.005 + 0.002i	Dutch Roll
0.005 - 0.002i	Dutch Roll
-0.0002 + 0.0002i	Pitch mode
-0.0002 - 0.0002i	Pitch mode

Table 14: Eigenvalues for Coupled Hover Stability

## 11.2 Tail Sizing

The tail rotor is typically sized by stability analysis to ensure adequate dynamic stability in forward flight and for offloading the anti-torque requirement in high speed conditions. For the current design, tail rotor is sized based on the statistical data for existing coaxial helicopters for simplicity. The actual sizing can be done through stability consideration in detailed design. The horizontal tail area is 12.81 ft<sup>2</sup> and the vertical tail area is fixed at 9.15 ft<sup>2</sup>.

# 12 Avionics

Avionic systems include communications, navigation, the display and management of multiple systems, and the hundreds of systems that are fitted to aircraft to perform individual functions. The main subsystem is the Autonomous Aircraft navigation system which basically has the job of Localizing the Aircraft, Mapping the Surroundings, Planning a trajectory, and then executing the control actions to follow the trajectory. Other subsystems include on-board computer, Flight Display or Pilot Interface units and Power management System.

## 12.1 Autonomous Flight Navigating System

The Autonomous Flight Navigation System of Heimdall has two flight modes (fully autonomous and manual control) depending on the level of autonomy required by the mission. In the fully autonomous mode the Motion Planning System will give the tracking commands to the Flight Control System whereas in manual control mode the Motion Planning System will get deactivated and the pilot commands will be supplied directly to the Flight Control System. This means that the helicopter, like many unmanned air vehicle systems operating today, can complete the mission automatically but still places a human in the decision loop. The Aircraft Navigation System is divided into many subsystems such as:

- Aircraft Localization and Mapping System
- Motion Planning System
- Flight Control System

The Localization and Mapping System will give us the estimated pose of the helicopter and at the same time generate global maps of the surrounding environment which is necessary for mission automation. To make the aircraft fully autonomous the map will be converted to occupancy grid and then it will be passed to the Motion Planning System which will generate the trajectory for a particular mission. This trajectory will then be supplied to the Flight Control System which will execute the necessary series of blade/motor actuations to make the helicopter follow the trajectory. Thus, the whole mission from take-off, to hover and other manoeuvres and then to landing will become fully autonomous. All these calculations will be done on the on-board computer. The full architecture of the System is shown in Fig. 49.

### 12.1.1 Motion Planning System

Helicopter can independently move along the three directions. This makes, it holonomic with respect to linear motion. Also, this motion is non-deterministic that is a given sequence of actions may not

take the helicopter to the same state always. Therefore, the Markov Decision Process is a good choice as a probabilistic planning algorithm for helicopters. The solution to a Markov Decision Process is a set of actions that the Aircraft should take in each state to reach the goal also called as policy. A policy is technically a mapping from states to action space. In each state, a policy tells the Aircraft what to do next and to solve the planning we have to find an optimal policy that takes the Aircraft to the goal with maximum reward or minimum cost. To achieve this, first we find using an iterative approach the utility of each state in the occupancy grid map. The utility of a state is the immediate reward for that state and the expected utility of the next state, provided the aircraft chooses an optimal action. Once this is done all the aircraft needs to do is to follow the maximum utility states along its way to the goal.

### **12.1.2 Flight Control System**

Helicopter is a statically unstable vehicle and therefore it requires an efficient and robust flight control system to give it artificial stability and assist the pilot in flight. This system comprises of a control algorithm/Law which is present on the on-board computer, the feedback sensors and the actuators. The control algorithm takes the feedback from the sensors and performs the desired actuations as required by the pilot or the Motion planner depending on whether the helicopter is in full autonomous mode or manual control mode.

#### **12.1.2.1 Control Law**

Helicopters suffer from various control complexities such as: 1) under-actuated property, 2) inherent non-linearity within the dynamic model, and 3) coupling between the translational dynamics states and rotational dynamics states, and also 4) uncertainty in parameters like mass or Inertia (due to fuel consumption). To address these difficulties, we have employed a non-linear adaptive control technique with inner-outer loop structured tracking controller.

With six degrees of freedom (three translational and three rotational) and only four independent inputs (two collective and two cyclic rotor pitch angles), helicopters are severely underactuated. Therefore, the translation and rotational dynamics are coupled and they are also highly non-linear. Therefore, the control architecture have been divided into three loops, to get over the above mentioned problems. The outer loop takes care of the translation control of the helicopter and generates the necessary desired attitude information for the inner loop. Here, the Certainty Equivalence Adaptive Control method has been employed. This method takes care of the uncertainties/changes in mass and ensures that an estimate of the helicopters mass converges with the actual current mass of the helicopter.

The inner loop takes care of the attitude/rotational control of the helicopter and generates the necessary moments/torques that must be generated by the change of the combination of the collective and cyclic pitch angles of the rotors. These desired moments are supplied to the 3rd/innermost loop. Here, in the inner loop the Non Certainty Equivalence Adaptive Control method has been employed. This method takes care of the uncertainties/changes in the Inertia of the helicopter and ensures that attitude tracking is accurately achieved. The innermost loop takes care of the combination of the collective and cyclic pitch inputs of the four rotors. Here, a stable first order error dynamics control is employed which makes the current moments provided by the rotors converge to the desired moments as supplied by the inner loop. The full control architecture is depicted by the Fig. 50.

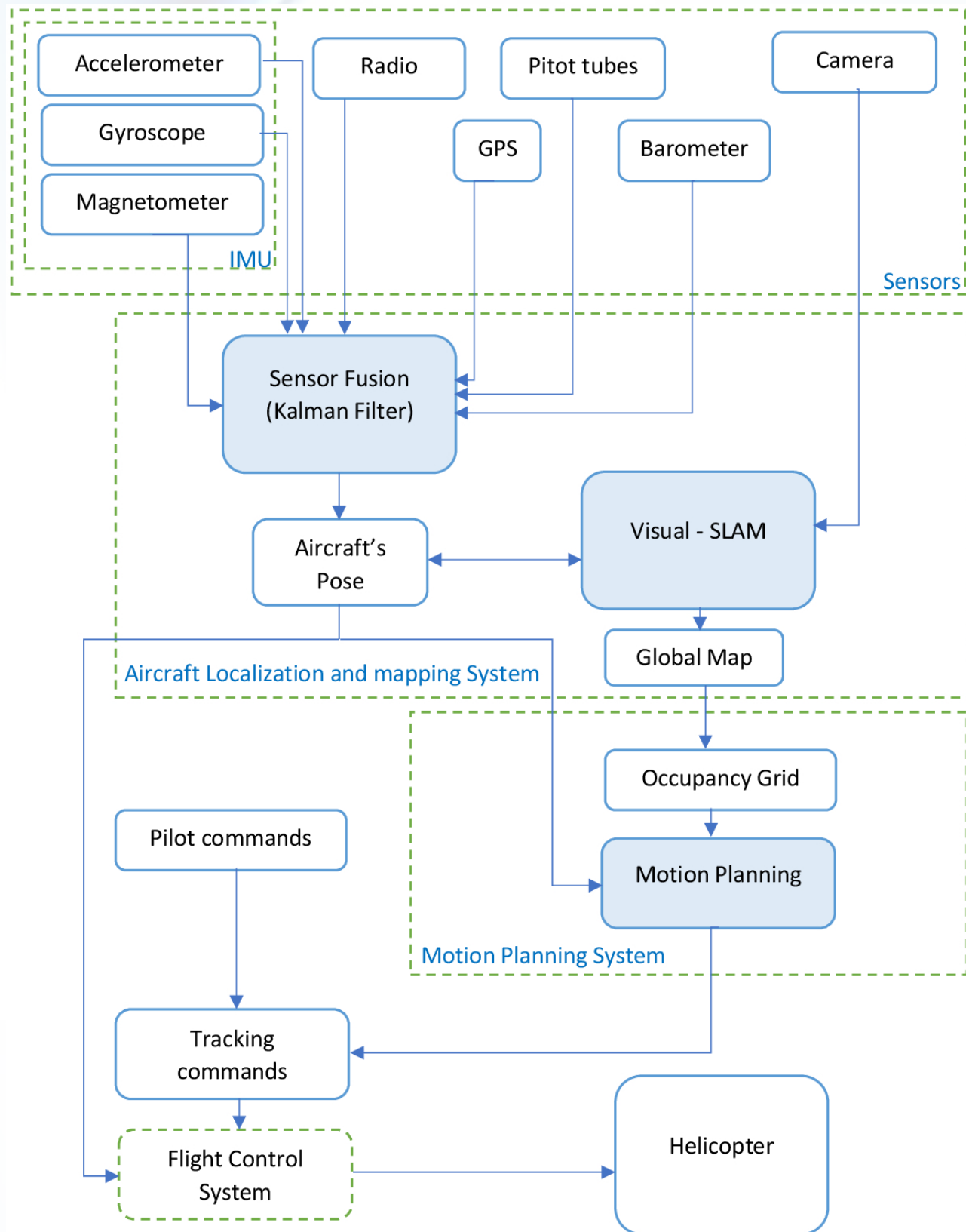


Figure 49: Autonomous Flight Navigation System Architecture

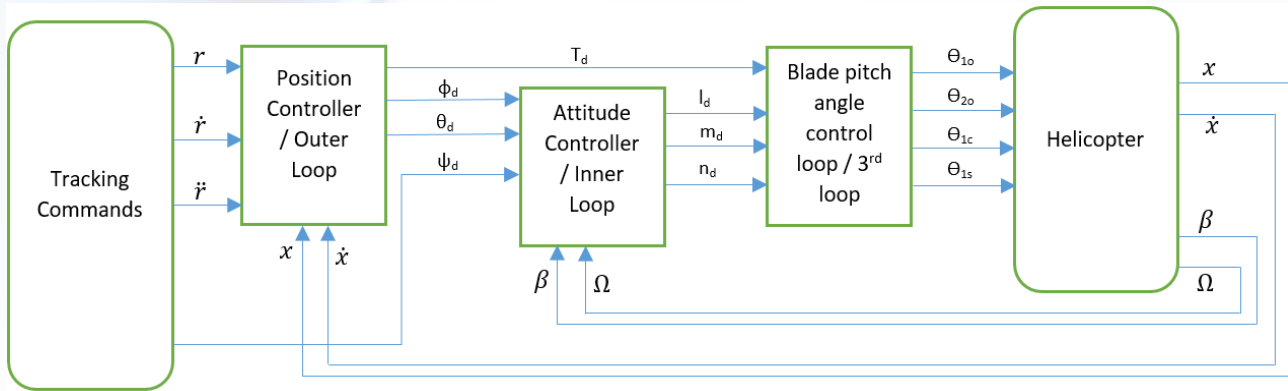


Figure 50: Control Architecture Block Diagram

## 12.2 Health and Usage Monitoring System (HUMS)

HUMS is a sensor-based monitoring system that enables Condition-Based Maintenance by measuring the health and performance of mission-critical components on aircraft. The HUMS of Heimdall does the following :

- Continuous vibration monitoring of drivetrain.
- Perform Rotor, Track and Balance.
- Provide actionable information for informed maintenance decisions.
- Pinpoint mechanical faults before they become catastrophic failures.

It also provides field-proven design and delivers specific, OEM-recommended maintenance actions to maintainers for rotor smoothing, engines and the entire drive train. For high processing speeds it has field-programmable gate arrays (FPGA). The HUMS system interfaces to hardwired vibration and tachometer sensors located throughout the aircraft and to the carry-on equipment such as the FasTrak Optical Tracker for Main Rotor blade tracking.

## 13 Weight Analysis

### 13.1 Weight Estimation

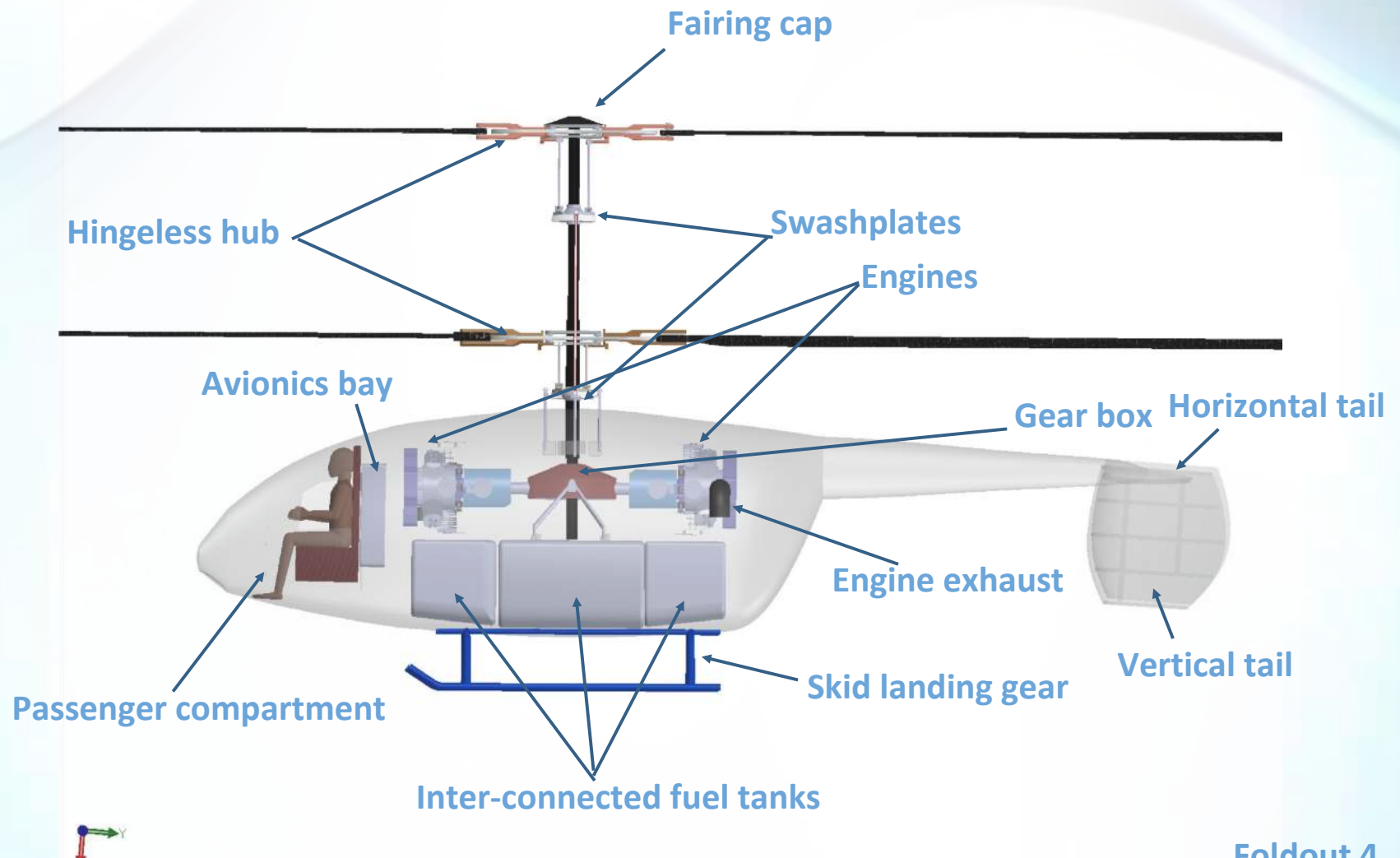
The weight estimation of most of the subsystems was done by Prouty's and Tishchenko's methods. For some subsystems like transmission system and landing gear, weights were calculated using CAD model and density of the material chosen for that respective subsystems. The Weight of these subsystems came to be much lesser than what was estimated using the Prouty's and Tishchenko's methodology. Hence the empty weight of Heimdall further decreased which also led to a decrease in the fuel weight, eventually decreasing the gross weight from the initially estimated weight of 5195 lbs. Lateral center of gravity(l.c.g) is referenced from the nose of the helicopter. Vertical centre of gravity(v.c.g) is referenced from the ground. The final weight breakdown of all the subsystems is mentioned in Table.15.

Description	Mass (lbs)	% Mass	I.c.g (mm)	v.c.g (mm)
Engine 1	337.3	15.05	1660	1486
Engine 2	337.3	15.05	3532	1486
Transmission system	225	10.04	2620	1536
Top rotor system	199.41	8.9	2620	4096
Bottom rotor system	210.33	9.39	2620	4096
Fuel system	81	3.61	2570	880
Landing gear	55	2.45	2540	13
Fuselage	343.93	15.35	2800	1086
Empennage	75	3.34	5200	1636
Tail	67.98	3.03	6680	1236
Control systems	11.43	0.51	1150	1100
Electrical systems	166.48	7.43	1170	936
APU	100	4.46	4000	1350
General furnishing	30	1.34	1000	1036
<b>Empty weight</b>	<b>2240.16</b>	<b>100</b>	<b>2770.86</b>	<b>1651.51</b>
Payload	176.37		900	1136
Transmission & Engine oil	15		2620	1550
Fuel	2061.3		2600	936
<b>Gross weight</b>	<b>4492.83</b>		<b>2618.53</b>	<b>1302.66</b>

Table 15: *Weight of individual subsystems of Heimdall*

Extreme values for the centre of gravity translation are 1.8 mm forward of the main rotor shaft and 12 mm aft of the shaft. These extreme values are well within the range of the controls. Various subsystems are shown according to their position in fuselage in foldout-4.

# Heimdall Inboard Profile



## 14 Cost Analysis

### 14.1 Acquisition Cost

The fundamental method used to estimate base purchase price of Heimdall is Harris and Scully method [21] a price estimating relationship that is based upon a linear regression statistical analysis of approximately 120 rotorcraft. This relatively simple empirical relationship is a function of empty weight, installed power, number of rotor blades, engine type, engine number, number of main rotors and type of landing gear. This global method is suitable for use in the preliminary stages of a design, due to the small number of required inputs. The cost of individual subsystems of Heimdall are given in the Table 16.

SAWE RP NO. 8A PART 1

GROUP WEIGHT STATEMENT

PAGE 1

NAME NIMBUS

USEFUL LOAD AND GROSS WEIGHT

MODEL HEIMDALL

DATE June 1, 2017

REPORT

	LOAD CONDITION						
115	WEIGHT EMPTY	2608.9					
117	UNUSABLE FUEL (TYPE____) (GALS____)	80					
119	TRAPPED	40					
121	ENGINE	674.6					
122	OPERATING WEIGHT						
150	PASS./TROOPS (QTY____) (WT.EA.____)						
151	CARGO	176.4					
153	ZERO FUEL WEIGHT						
164	USABLE FUEL TYPE LOC GAL	2050.3					
165	TOTAL USEFUL LOAD						
170	GROSS WEIGHT	4560.1					
171							

### 14.2 Reasons for low cost

- **Structural simplicity:** The component design is structured in such a way that It is easier to manufacture and minimize the manufacturing cost.
- **Balance between maturity and readiness:** Throughout the analysis of the design, consistent emphasis was put on a balance between existing and future technology. Incorporation of variable radius rotors ensures that the Heimdall is an attractive option in the coming market.
- **Placement of components:** While considering positions of various components, extra care was taken for accessibility, in order to ease the maintenance cost.

Components	Cost as per 2002 (USD)	Cost in the year 2017 (USD)
Rotor system	67365	91562
Airframe structure	226163	307401
Landing gear	4177	5677
Engine installation	90330	12277
Powerplant structure	30058	40855
Drive system	53481	72691
Control system	1159	1575
Electrical systems	22916	31147
Avionics	28161	38276
General furnishing	2374	3227
Assembly	124192	168801
<b>Manufacturing cost</b>	<b>650375</b>	<b>883990</b>
Tooling amortization and profit	325187	441995
<b>Base price</b>	<b>975562</b>	<b>1325984</b>

Table 16: *Cost of individual subsystems of Heimdall*

## 15 Conclusion

Heimdall is the answer to hover for a day challenge. With its unique, innovative rotor system with un-equal top and bottom rotors, require very low power for hover. The innovative coaxial rotor combined with the state-of-the-art high efficiency diesel engine enables hovering continuously for 24 hours possible. The coaxial rotor system allows for use of blades with large radius and very low disc loading enabling high efficiency hover.

## References

- [1] Saaty, T.L., “Multi-criteria Decision Making: The Analytic Hierarchy Process”, RWS Publications, Pittsburgh, PA, 1990.
- [2] Leishman, J. G., “Principles of Helicopter Aerodynamics”, Cambridge University Press, Cambridge, 2000.
- [3] Harrington, R. D., “Full-Scale-Tunnel Investigation of the Static Thrust Performance of a Coaxial Helicopter Rotor”, NACA Technical Note 2318, 1951.
- [4] Bailey, F. J., Jr., “A Simplified Theoretical Method of Determining the Characteristics of a Lifting Rotor in Forward Flight”, NACA Technical Report 716, 1941.
- [5] Kim, H. W., and Brown, R. E., “A Comparison of Coaxial and Conventional Rotor Performance”, Journal of the American Helicopter Society, Vol. 55, No. 1, 2010, pp. 12004-12004.
- [6] Prouty, R. W., “Helicopter Performance, Stability and Control”, Kreiger Publishing Company, Malabar, Florida 1995.

- [7] Leishman, J. G., and Syal, M., “Figure of Merit Definition for Coaxial Rotors,” Journal of the American Helicopter Society, Vol. 53, No. 3, 2008, pp. 290–300.
- [8] Unsworth, D. K., and Sutton, J. G., “An Assessment of the Impact of Technology on VTOL weight Prediction” Proceedings of the 40<sup>th</sup> Annual American Helicopter Society Forum, 1984.
- [9] Reisdorfer, D., and Thomas, M. L., “Static Test and Flight Test of the Army/Bell ACAP Helicopter”, Proceedings of the 42<sup>nd</sup> Annual American Helicopter Society Forum, June 1986
- [10] Snyder, C. A., “Personal Rotorcraft Design and Performance with Electric Hybridization,” Proceedings of 73rd American Helicopter Society Annual Forum, Fort Worth, TX, USA, May 9-11, 2017.
- [11] Bourtsev, B. N., Selemenev, S. V., and Vagis, V. P., “Coaxial Helicopter Rotor Design and Aeromechanics”, Proceedings of 25th European Rotorcraft Forum, Rome, Italy, September 14-16, 1999.
- [12] Totah, J., “A Critical Assessment of UH-60 Main Rotor Blade Airfoil Data”, American Institute of Aeronautics and Astronautics, 1993. AIAA-1993-3413.
- [13] Syal, M., and Leishman, J. G., “Aerodynamic Optimization Study of a Coaxial Rotor in Hovering Flight”, Journal of the American Helicopter Society 57, 042003 (2012)
- [14] Wicha, Jan., “Coaxial rotor hover power reduction using dissimilarity between upper and lower rotor design”, Masters Thesis, Rensselaer Polytechnic Institute, July 2015
- [15] Zoche engine brochure, [www.zoche.de/zuche\\_brochure.pdf](http://www.zoche.de/zuche_brochure.pdf)
- [16] Automated Dynamics, [www.automateddynamics.com](http://www.automateddynamics.com)
- [17] Maciejczyk, A., and Zdziennicki, Z., “Design basic of industrial gear boxes” Department of Vehicles and Fundamentals of Machine Design, Technical University of Lodz.
- [18] ”Engineering Design Handbook, Helicopter Engineering, Part One – Preliminary Design”, Army Material Command, Alexandria, Virginia, August 30, 1974.
- [19] Rawal, N., and Abhishek , “Modelling and Analysis of a Coaxial Tiltrotor” 4th Asian/Australian Rotorcraft Forum, IISc, India, November 1618, 2015
- [20] Jakob Engel, Thomas Schops and Daniel Cremers., “Large-Scale Direct Monocular SLAM”, Proceedings of European Conference on Computer Vision (ECCV), 2014.
- [21] Harris and Scully, “Helicopters Cost Too Much”, Proceedings of 53rd American Helicopter Society Annual Forum, May 1997, pp 1575–1608.